Classical and Bayesian Inference of Engineering and Disability Data: Using the Kavya Manoharan Power Chris-Jerry Distribution under Hybrid Censoring

Abdullah Ali H. Ahmadini[1], Ahmed R. El-Saeed[2,3], Ehab M. Almetwally[2] and Mohammed Elgarhy[4,*]

[1] Department of Mathematics, College of Science, Jazan University, Jazan, 45142, Saudi Arabia

[2] Department of Mathematics and Statistics, College of Science, Imam Mohammad Ibn Saud Islamic University (IMSIU), Riyadh, 11432, Saudi Arabia

[3] King Salman Center for Disability Research, Riyadh, 11614, Saudia Arabia

[4] Department of Basic Sciences, Higher Institute of Administrative Sciences, Belbeis, 44621, Egypt

INFORMATION

Keywords:
Kavya-Manoharan family
power Chris-Jerry
moments
hybrid censoring
bayesian
engineering
disability
maximum likelihood estimation

DOI: 10.23967/j.rimni.2025.10.72440

SCIPEDIA
Revista Internacional de Métodos Numéricos para Cálculo y Diseño en Ingeniería
RIMNI

Classical and Bayesian Inference of Engineering and Disability Data: Using the Kavya Manoharan Power Chris-Jerry Distribution under Hybrid Censoring

Abdullah Ali H. Ahmadini[1], **Ahmed R. El-Saeed**[2,3], **Ehab M. Almetwally**[2] **and Mohammed Elgarhy**[4,*]

[1]Department of Mathematics, College of Science, Jazan University, Jazan, 45142, Saudi Arabia

[2]Department of Mathematics and Statistics, College of Science, Imam Mohammad Ibn Saud Islamic University (IMSIU), Riyadh, 11432, Saudi Arabia

[3]King Salman Center for Disability Research, Riyadh, 11614, Saudia Arabia

[4]Department of Basic Sciences, Higher Institute of Administrative Sciences, Belbeis, 44621, Egypt

ABSTRACT

In this article, we study and introduce the Kavya-Manoharan power Chris-Jerry distribution (KMPCJD) which is a new generation of the power Chris-Jerry distribution (PCJD) which is suitable for engineering and disability data. The probability density curves of KMPCJD demonstrate that it has practical applications in analyzing engineering and disability data in Saudi Arabia. Researchers have a lot of flexibility when developing statistical models for research on disability issues, since the hazard rate function (HRF) for KMPCJD can exhibit J-shaped, increasing, and decreasing trends. In addition, several significant KMPCJD features are calculated, including moments, reliability metrics, moment-generating function, and order statistics. Using data on engineering and disability difficulties, we estimate the parameters of KMPCJD and use classical and Bayesian techniques to assess their reliability and HRF under hybrid censored schemes. Asymptotic confidence/credible intervals are calculated. The numerical results show that when the sample size n increases while keeping other factors like r and T constant, the estimators for δ and λ show improved performance in terms of reduced Bias, mean square error (MSE), and narrower confidence intervals. Also, the Bayesian method also produces shorter credible intervals (LCCI) compared to the traditional confidence intervals (LACI) from ML and MPS methods, suggesting higher precision. To show the utility of the suggested distribution, it was tested in five datasets related to engineering and disability issues in Saudi Arabia. The KMPCJD performed better in terms of goodness of fit than a number of models, including the Kavya Manoharan Rayleigh inverted Weibull distribution, Kavya Manoharan Burr X distribution, exponentiated generalized power Lindley distribution, Weibull power Lindley distribution, power Lindley distribution, Kavya Manoharan generalized exponential distribution, power XLindley distribution, Kavya Manoharan unit exponentiated half logistic distribution, and PCJD. Due to its superior fit capabilities, the KMPCJD is suggested for data modeling in disciplines including engineering and disability difficulties.

OPEN ACCESS

Received: 27/08/2025

Accepted: 19/09/2025

Published: 27/11/2025

DOI
10.23967/j.rimni.2025.10.72440

Keywords:
Kavya-Manoharan family
power Chris-Jerry
moments
hybrid censoring
bayesian
engineering
disability
maximum likelihood estimation

*Correspondence: Mohammed Elgarhy (dr.moelgarhy@gmail.com).

1 Introduction

In a wide range of fields, including public health, administration, engineering, medicine, and biological sciences, lifetime data are important. To analyze these key data features, statistical distributions are employed to model them. A suitable distribution might yield important data that helps in making judgments and conclusions. A growing number of academics are employing the new, more generalized distributions when they are required to be more adaptable. The one-parameter life-time distribution known as the Chris-Jerry distribution (CJD), due to Onyekwere and Obulezi [1], is becoming more and more well known in the statistical literature. This is because it fits a wider range of data sets more accurately than a number of Lindley classes of distributions (Rama, Shanker, Rani, Pranav, Akash, Aradhana, Sujatha, Ishita, xgamma, and Lindley). Several authors discussed extended and generalized forms of CJD, such as Kumaraswamy CJD [2], power size biased CJD [3], Marshall-Olkin CJD [4], power CJD [5], shifted CJD [6] and two-parameter mixture CJD [7].

Our focus here is on an important generalization of the CJD with an additional shape parameter, known as power CJD (PCJD). The probability density function (PDF) of the PCJD with shape parameter $\delta > 0$, and scale parameter $\lambda > 0$, is as follows:

$$g(x;\delta,\lambda) = \frac{\delta\lambda^2 x^{\delta-1} e^{-\lambda x^\delta}(\lambda x^{2\delta}+1)}{\lambda+2}; \quad x > 0. \tag{1}$$

The cumulative distribution function (CDF) and hazard rate function (HRF) of the PCJD are given, respectively, by

$$G(x;\delta,\lambda) = 1 - e^{-\lambda x^\delta}\left(\frac{\lambda x^\delta(\lambda x^\delta+2)}{\lambda+2}+1\right); \quad x > 0, \tag{2}$$

and

$$h(x;\delta,\lambda) = \frac{\delta\lambda^2 x^{\delta-1}(\lambda x^{2\delta}+1)}{\lambda^2 x^{2\delta}+2\lambda x^\delta+\lambda+2}.$$

The addition of parameters enhances flexibility, however simultaneously presents the challenge of assessing their complexity. Recently, the Kavya-Manoharan (KM) transformation family of distributions was examined by [8]. The associated CDF and PDF are presented through

$$F(x;\zeta) = \frac{e}{e-1}\left(1-e^{-G(x;\zeta)}\right), x \in \mathbb{R}, \tag{3}$$

and

$$f(x;\zeta) = \frac{e}{e-1} g(x;\zeta) e^{-G(x;\zeta)}, \tag{4}$$

where $g(x;\zeta)$, $G(x;\zeta)$ are the PDF and CDF of the baseline distribution and ζ is the vector of parameter.

In order to generate lifetime models or distributions, this family uses a baseline distribution that has been provided. Rather than adding more parameters to the model to maintain its adaptability to the present uncertainty, they are concentrating on estimating the lifetime by employing a method that produces accurate and minimal results. Many authors used the KM family to generate new distributions such as new lifetime model [9], Kavya-Manoharan log-logistic model [10], arctan Kavya-Manoharan-G class of distributions [11], Kavya-Manoharan Bilal distribution [12], and generalized Kavya-Manoharan-G family of distributions [13]. In this article, our objective was to construct a new lifespan model for survival analysis, the Kavya-Manoharan power Chris-Jerry (KMPCJD), by compounding the KM class and the PCJD.

Hybrid censoring is an experimental design that terminates a life test at the earlier of a prespecified time T or the occurrence of the r-th failure; the stopping rule is therefore

$$\tau = \min\{T, x_{r:n}\}, \tag{5}$$

where $x_{1:n} < x_{2:n} < \cdots < x_{n:n}$ denote the ordered lifetimes. This mixed censoring scheme combines the practical advantages of time-truncation and failure-truncation: it permits control over the duration and cost of an experiment while ensuring a minimum amount of failure information for reliable inference. From a statistical viewpoint, hybrid censoring alters the likelihood structure and complicates standard inferential procedures developed for pure Type-I or Type-II censoring, thereby motivating tailored approaches such as modified maximum-likelihood estimators, product-spacing methods, Bayesian estimation via MCMC, and resampling- or simulation-based assessments of finite-sample behavior. The design is particularly relevant in reliability engineering, industrial life-testing and medical survival studies where either calendar time or a required number of events constrains experimentation. Methodological contributions over the past decades have developed both likelihood and Bayesian treatments for hybrid schemes and their progressive/adaptive extensions.

More paper used and discussed hybrid censoring as: Statistical analysis of alpha power inverse Weibull distribution under hybrid censored scheme has been obtained by [14]. Statistical analysis of alpha-power exponential distribution using unified hybrid censored has been introduced by [15]. Classical and Bayesian inference for the Kavya-Manoharan generalized exponential distribution (KMGED) under generalized progressively hybrid censored has been obtained by [16]. Statistical analysis of inverse Weibull based on step-stress partially accelerated life tests with unified hybrid censoring data has been discussed by [17]. Analysis of uncertainty measure using unified hybrid censored data has been introduced by [18]. Point and interval estimation of reliability and entropy for generalized exponential distribution under generalized type-II Hybrid censoring scheme has been discussed by [19].

This study aims to analyze engineering data and the distribution of individuals with disabilities in Saudi Arabia based on key variables such as administrative regions, gender, and age groups. By identifying regional and demographic trends, this research seeks to uncover disparities and inform policy measures aimed at improving accessibility and healthcare services for people with disabilities. The findings offer crucial insights that can guide resource allocation and the implementation of targeted support programs. In this paper we adopt the hybrid censoring framework above and concentrate on the development and comparison of parameter estimation procedures, supported by simulation studies illustration.

The remainder of the paper is organized in the following manner: Section 2 provides a precise definition of the KMPCJD. Section 3 explores several dependability metrics. In Section 4, we describe a range of statistical aspects of the KMPCJD. The procedure for estimating the model parameters using maximum likelihood is described in Section 5. Section 6 discusses the outcomes of the simulation research. Section 7 concludes by showcasing the practical applications of the KMPCJD model using five real data sets related to engineering and disability. This serves to highlight the significance of the newly suggested model. The paper's conclusion is presented in Section 8.

2 The New KMPCJD

In this section, we formulate the flexible KMPCJD by inserting (2) into (3). Then we get the CDF of the KMPCJD as follows:

$$F(x;\delta,\lambda) = \frac{e}{e-1}\left(1 - e^{-\left(1-e^{-\lambda x^{\delta}}\left(\frac{\lambda x^{\delta}(\lambda x^{\delta}+2)}{\lambda+2}+1\right)\right)}\right), \quad x > 0, \quad \delta,\lambda > 0, \tag{6}$$

and the corresponding PDF can be constructed by utilizing (1) and (2) into (4) as below

$$f(x;\delta,\lambda) = \frac{e}{e-1}\left(\frac{\delta\lambda^{2}x^{\delta-1}e^{-\lambda x^{\delta}}(\lambda x^{2\delta}+1)}{\lambda+2}\right)e^{-\left(1-e^{-\lambda x^{\delta}}\left(\frac{\lambda x^{\delta}(\lambda x^{\delta}+2)}{\lambda+2}+1\right)\right)}. \tag{7}$$

Fig. 1 shows some curves of the PDF and CDF for the KMPCJD. We can note that in Fig. 1, the PDF curves for KMPCJD can be left-skewed, unimodal, right-skewed, and decreasing. Also from Fig. 1, the CDF plot of the KMPCJD exhibits an increasing curve, starting near zero, gradually increasing, and then approaching one as the variable increases.

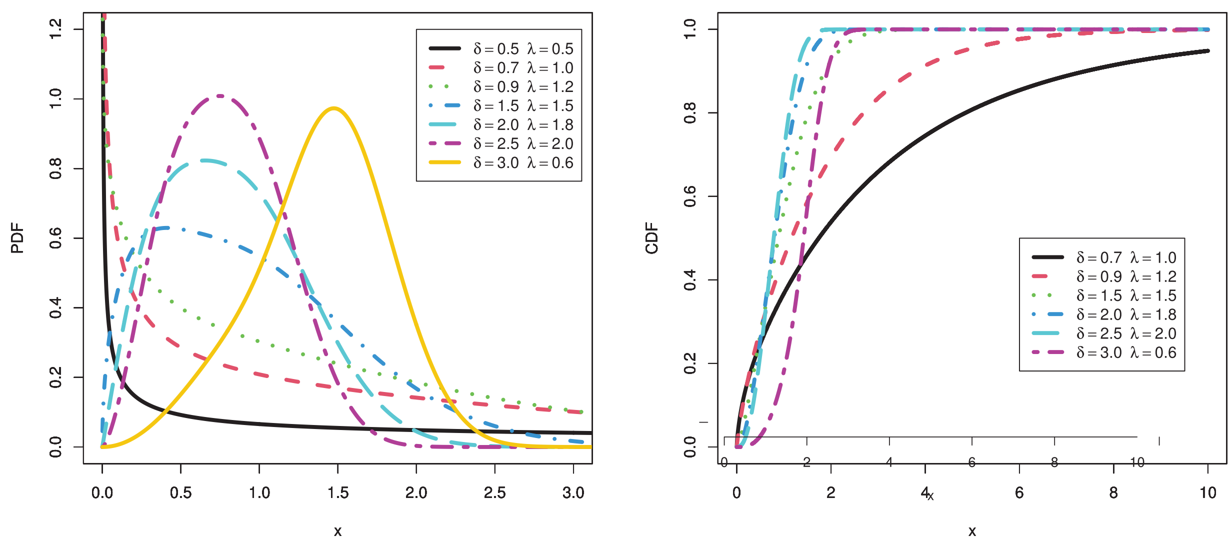

Figure 1: Plots of the PDF and CDF for the KMPCJD

3 Reliability Measures

In this section, we discuss some reliability measures for the KMPCJD. The survival function (SF) and HRF for KMPCJD are provided by

$$S(x;\delta,\lambda) = 1 - \frac{e}{e-1}\left(1 - e^{-\left(1-e^{-\lambda x^{\delta}}\left(\frac{\lambda x^{\delta}(\lambda x^{\delta}+2)}{\lambda+2}+1\right)\right)}\right), \quad x > 0, \quad \delta,\lambda > 0,$$

and

$$h(x;\delta,\lambda) = \frac{\frac{e}{e-1}\left(\frac{\delta\lambda^{2}x^{\delta-1}e^{-\lambda x^{\delta}}(\lambda x^{2\delta}+1)}{\lambda+2}\right)e^{-\left(1-e^{-\lambda x^{\delta}}\left(\frac{\lambda x^{\delta}(\lambda x^{\delta}+2)}{\lambda+2}+1\right)\right)}}{1 - \frac{e}{e-1}\left(1 - e^{-\left(1-e^{-\lambda x^{\delta}}\left(\frac{\lambda x^{\delta}(\lambda x^{\delta}+2)}{\lambda+2}+1\right)\right)}\right)}.$$

The reversed HRF (RHRF) and cumulative HRF (CHRF) for KMPCJD are provided by

$$\tau(x;\delta,\lambda)=\frac{\left(\dfrac{\delta\lambda^{2}x^{\delta-1}e^{-\lambda x^{\delta}}\left(\lambda x^{2\delta}+1\right)}{\lambda+2}\right)e^{-\left(1-e^{-\lambda x^{\delta}}\left(\frac{\lambda x^{\delta}\left(\lambda x^{\delta}+2\right)}{\lambda+2}+1\right)\right)}}{1-e^{-\left(1-e^{-\lambda x^{\delta}}\left(\dfrac{\lambda x^{\delta}\left(\lambda x^{\delta}+2\right)}{\lambda+2}+1\right)\right)}}$$

and

$$H(x;\delta,\lambda)=-\log\left[1-\frac{e}{e-1}\left(1-e^{-\left(1-e^{-\lambda x^{\delta}}\left(\frac{\lambda x^{\delta}\left(\lambda x^{\delta}+2\right)}{\lambda+2}+1\right)\right)}\right)\right].$$

Figs. 2 and 3 show some curves of HRF, SF, RHRF and CHRF for the KMPCJD. We can note that in Fig. 2 the HRF curves for KMPCJD can be J-shaped, increasing, and decreasing. In addition we can note from Fig. 3, the RHRF is decreasing, but the CHRF can be increasing or J-shaped.

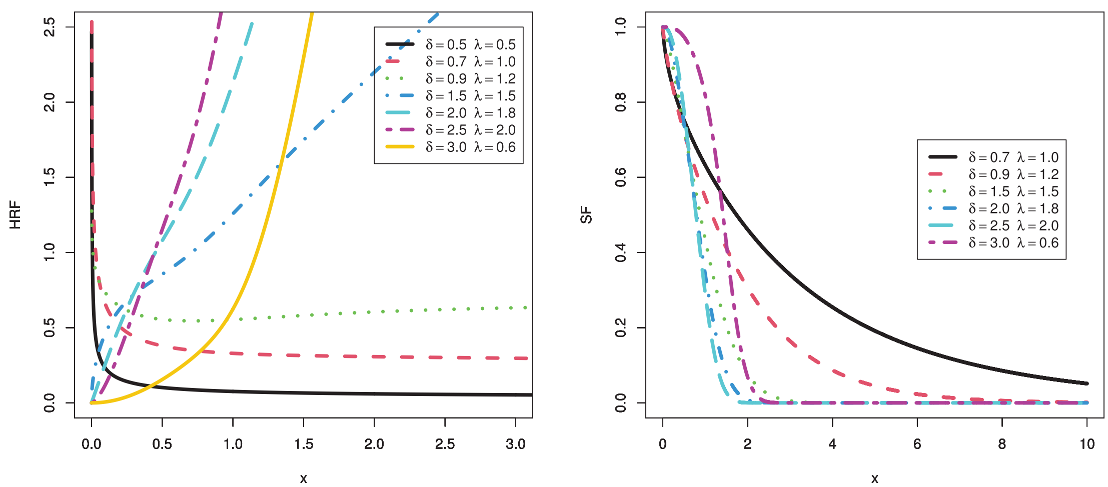

Figure 2: Plots of HRF and SF for the KMPCJD

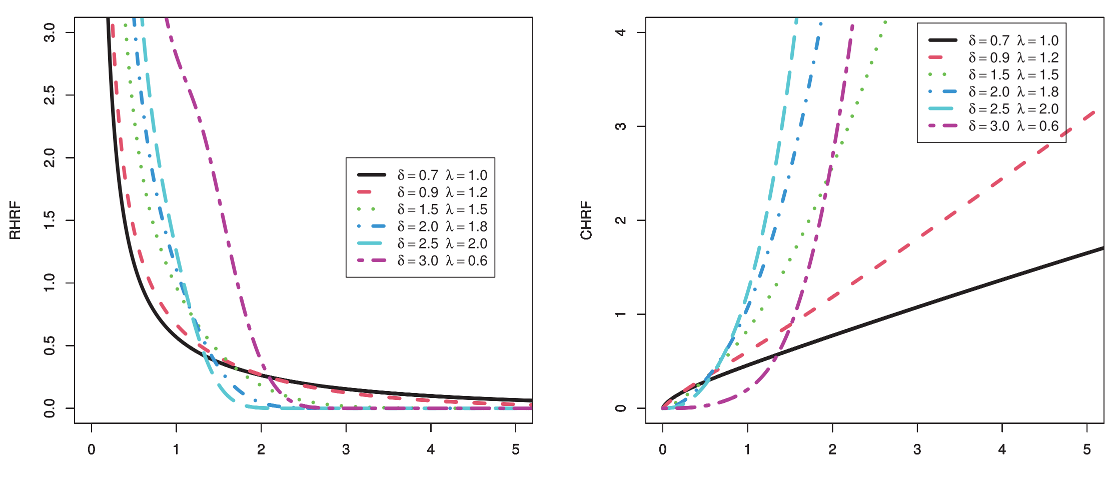

Figure 3: Plots of RHRF and CHRF for the KMPCJD

4 Statistical Measures

This section focuses on the analysis of significant statistical metrics of the KMPCJD.

4.1 Moments

The r_{th} moment of a random variable X with KMPCJD is provided by

$$\mu'_r = E(X^r) = \int_0^\infty x^r f(x;\lambda,\delta)dx$$

$$= \frac{\delta\lambda^2 e}{(e-1)(\lambda+2)}\int_0^\infty x^{r+\delta-1}e^{-\lambda x^\delta}(1+\lambda x^{2\delta})e^{-\left(1-e^{-\lambda x^\delta}\left(\frac{\lambda x^\delta(\lambda x^\delta+2)}{\lambda+2}+1\right)\right)}dx. \tag{8}$$

Using the exponential series $e^{-ax} = \sum_{i=0}^{\infty}(-1)^i\frac{a^i}{i!}x^i$ in the above equation, we have

$$\mu'_r = \frac{\delta\lambda^2 e}{(e-1)(\lambda+2)}\sum_{i=0}^{\infty}\frac{(-1)^i}{i!}\int_0^\infty x^{r+\delta-1}e^{-\lambda x^\delta}\left(1+\lambda x^{2\delta}\right)\left(1-e^{-\lambda x^\delta}\left(1+\frac{\lambda x^\delta(\lambda x^\delta+2)}{\lambda+2}\right)\right)^i dx.$$

By employing the binomial expansion to the last term of the above equation

$$\left(1-e^{-\lambda x^\delta}\left(1+\frac{\lambda x^\delta(\lambda x^\delta+2)}{\lambda+2}\right)\right)^i = \sum_{j=0}^{i}(-1)^j\binom{i}{j}e^{-j\lambda x^\delta}\left(1+\frac{2\lambda x^\delta(1+0.5\lambda x^\delta)}{\lambda+2}\right)^j,$$

we get

$$\mu'_r = \frac{\delta\lambda^2 e}{(e-1)(\lambda+2)}\sum_{i=0}^{\infty}\sum_{j=0}^{i}\frac{(-1)^{i+j}}{i!}\binom{i}{j}\int_0^\infty x^{r+\delta-1}e^{-(j+1)\lambda x^\delta}\left(1+\lambda x^{2\delta}\right)\left(1+\frac{2\lambda x^\delta(1+0.5\lambda x^\delta)}{\lambda+2}\right)^j dx.$$

Again using the binomial expansion to the last term $\left(1+\frac{2\lambda x^\delta(1+0.5\lambda x^\delta)}{\lambda+2}\right)^j = \sum_{k=0}^{j}\binom{j}{k}\frac{2^k\lambda^k}{(\lambda+2)^k}x^{k\delta}(1+0.5\lambda x^\delta)^k$, we have

$$\mu'_r = \frac{\delta e}{(e-1)}\sum_{i=0}^{\infty}\sum_{j=0}^{i}\sum_{k=0}^{j}\frac{(-1)^{i+j}}{i!}\binom{i}{j}\binom{j}{k}\frac{2^k\lambda^{k+2}}{(\lambda+2)^{k+1}}\int_0^\infty x^{r+(k+1)\delta-1}e^{-(j+1)\lambda x^\delta}\left(1+\lambda x^{2\delta}\right)\left(1+0.5\lambda x^\delta\right)^k dx.$$

By employing the binomial expansion $(1+0.5\lambda x^\delta)^k = \sum_{l=0}^{k}\binom{k}{l}2^{-l}\lambda^l x^{l\delta}$ to the last term in the above equation, we get

$$\mu'_r = \frac{\delta e}{(e-1)}\sum_{i=0}^{\infty}\sum_{j=0}^{i}\sum_{k=0}^{j}\sum_{l=0}^{k}\frac{(-1)^{i+j}}{i!}\binom{i}{j}\binom{j}{k}\binom{k}{l}\frac{2^{k-l}\lambda^{k+l+2}}{(\lambda+2)^{k+1}}\int_0^\infty x^{r+(k+l+1)\delta-1}\left(1+\lambda x^{2\delta}\right)e^{-(j+1)\lambda x^\delta}dx.$$

Let $y = (j+1)\lambda x^{\delta}$, then

$$\mu_r' = \frac{e}{(e-1)} \sum_{i=0}^{\infty} \sum_{j=0}^{i} \sum_{k=0}^{j} \sum_{l=0}^{k} \binom{i}{j} \binom{j}{k} \binom{k}{l} \frac{(-1)^{i+j} 2^{k-l} \lambda^{1-\frac{r}{\delta}}}{(\lambda+2)^{k+1} i!\,(j+1)^{\frac{r}{\delta}+(k+l+1)}} \int_0^{\infty} y^{\frac{r}{\delta}+k+l} \times \left(1 + \frac{y^2}{(j+1)^2 \lambda}\right) e^{-y} dy.$$

The moment r_{th} of the KMPCJD is

$$\mu_r' = \sum_{i=0}^{\infty} \sum_{j=0}^{i} \sum_{k=0}^{j} \sum_{l=0}^{k} \binom{i}{j} \binom{j}{k} \binom{k}{l} \frac{(-1)^{i+j} 2^{k-l} \lambda^{1-\frac{r}{\delta}} e}{(e-1)(\lambda+2)^{k+1} i!\,(j+1)^{\frac{r}{\delta}+k+l+1}} \times \left[\Gamma\left(\frac{r}{\delta}+k+l+1\right) + \frac{\Gamma\left(\frac{r}{\delta}+k+l+3\right)}{(j+1)^2 \lambda}\right].$$

4.2 The Moment Generating Function

The moment generating function of a random variable X with KMPCJD is provided by

$$M_x(t) = E\left(e^{tX}\right) = \sum_{r=0}^{\infty} \frac{t^r}{r!} \mu_r'$$
$$= \sum_{i=0}^{\infty} \sum_{j=0}^{i} \sum_{k=0}^{j} \sum_{l=0}^{k} \sum_{r=0}^{\infty} \binom{i}{j} \binom{j}{k} \binom{k}{l} \frac{(-1)^{i+j} 2^{k-l} \lambda^{1-\frac{r}{\delta}} t^r e}{(e-1)(\lambda+2)^{k+1} r!\, i!\,(j+1)^{\frac{r}{\delta}+k+l+1}} \times \left[\Gamma\left(\frac{r}{\delta}+k+l+1\right) + \frac{\Gamma\left(\frac{r}{\delta}+k+l+3\right)}{(j+1)^2 \lambda}\right].$$

4.3 Order Statistics

Assume that $X_1, X_2, \ldots, X_n$ is a random sample of KMPCJD with order statistics (OS) $X_{(1)}, X_{(2)}, \ldots, X_{(n)}$. The PDF of $X_{(m)}$ of OS is provided via

$$f_{X_{(m)}}(x) = \frac{n!}{(m-1)!\,(n-m)!} f(x;\lambda,\delta)[F(x;\lambda,\delta)]^{m-1}[1-F(x;\lambda,\delta)]^{n-m}. \tag{9}$$

The PDF of $X_{(m)}$ can be calculated as follows:

$$f_{X_{(m)}}(x) = \frac{n! e^m}{(m-1)!\,(n-m)!(e-1)^m} \left(\frac{\delta\lambda^2 x^{\delta-1} e^{-\lambda x^{\delta}} (\lambda x^{2\delta}+1)}{\lambda+2}\right) \Xi^*[1-\Xi^*]^{m-1} \left[1 - \frac{e}{e-1}(1-\Xi^*)\right]^{n-m}, \tag{10}$$

where $\Xi^* = e^{-\left(1-e^{-\lambda x^{\delta}}\left(\frac{\lambda x^{\delta}(\lambda x^{\delta}+2)}{\lambda+2}+1\right)\right)}$. The PDF of the smallest and largest OS for the KMPCJD can be computed by setting $m=1$ and $m=n$ in (10) as follows:

$$f_{X_{(1)}}(x) = \frac{ne}{(e-1)} \left(\frac{\delta\lambda^2 x^{\delta-1} e^{-\lambda x^{\delta}} (\lambda x^{2\delta}+1)}{\lambda+2}\right) \Xi^* \left[1 - \frac{e}{e-1}(1-\Xi^*)\right]^{n-1},$$

and

$$f_{X_{(n)}}(x) = \frac{ne^n}{(e-1)^n}\left(\frac{\delta\lambda^2 x^{\delta-1} e^{-\lambda x^\delta}(\lambda x^{2\delta}+1)}{\lambda+2}\right)\Xi^*[1-\Xi^*]^{n-1}.$$

5 Statistical Inference under Hybrid Censoring

This section delineates the attributes of hybrid censoring samples utilized in the study. Three distinct estimation methods are proposed to derive the point estimators for the parameters δ and λ, as well as the SF and HRF of the KMPCJD. Interval estimators, including ACI and HPD credible intervals, are generated.

5.1 Hybrid Censoring Description

A widely recognized experimental design termed hybrid censoring concludes the test upon reaching a predetermined number of failures r or a certain duration T. In this study, we examine n test units, with their lifetimes denoted as $x_{1:n} < x_{2:n} < \cdots < x_{n:n}$, which follow a probability density function $f(x;\Omega)$, where Ω represents a vector of unknown parameters. Three categories of observations are possible due to the experiment concluding at $\tau = \min(T; x_{r:n})$. The recorded lifespan under this censorship can thus be categorized as:

- **Type-I censoring:** Occurs when the first d ordered observations $x_{1:n}, x_{2:n}, \ldots, x_{d:n}$ are observed, with $d < r$, and the censoring time T lies between $x_{d:n}$ and $x_{d+1:n}$; that is, $x_{d:n} < T < x_{d+1:n}$.
- **Type-II censoring:** Takes place when the experiment continues until r failures are observed, i.e., $x_{1:n}, x_{2:n}, \ldots, x_{r:n}$, with the r-th failure occurring before the censoring time T, so $x_{r:n} < T$.
- **Complete data:** All n observations $x_{1:n}, x_{2:n}, \ldots, x_{n:n}$ are recorded before the censoring time T, i.e., $x_{n:n} < T$, and the total number of observations equals r, so $n = r$.

It is important to note that d denotes the count of failures recorded prior to the designated period T.

The likelihood function for a censored hybrid sample $x_{1:n} < x_{2:n} < \cdots < x_{d:n}$, adhering to a distribution with PDF $f(x;\Omega)$ and CDF $F(x;\Omega)$, is articulated as follows:

$$L(\Omega) \propto [1 - F(\tau;\Omega)]^{n-d}\prod_{i=1}^{d} f(x_{i:n};\Omega). \tag{11}$$

5.2 Maximum Likelihood Method

A proficient method for estimating the parameter Ω, where $\Omega = (\delta,\lambda)^T$, SF and HRF of the KMPCJD, is the maximum likelihood estimation [20–22] approach. Let $x_{1:n}, x_{1:n}, \ldots, x_{d:n}$ represent a hybrid censored sample derived from the PDF (7) and CDF (6). The likelihood function for the parameter set and observed samples is established according to Eq. (11) as follows:

$$\begin{aligned} l(\underline{\mathbf{x}}\,|\Omega) = {} & \left(1 - \frac{e}{e-1}\left(1 - e^{-\left(1-e^{-\lambda\tau^\delta}\left(\frac{\lambda\tau^\delta(\lambda\tau^\delta+2)}{\lambda+2}+1\right)\right)}\right)\right)^{n-d}\prod_{i=1}^{d}\left(\frac{\delta\lambda^2 x_{i:n}^{\delta-1} e^{-\lambda x_{i:n}^\delta}(\lambda x_{i:n}^{2\delta}+1)}{\lambda+2}\right) \\ & \times\left(\frac{e}{e-1}\right)^{d} e^{-\sum_{i=1}^{d}\left(1-e^{-\lambda x_{i:n}^\delta}\left(\frac{\lambda x_{i:n}^\delta(\lambda x_{i:n}^\delta+2)}{\lambda+2}+1\right)\right)}. \end{aligned} \tag{12}$$

The logarithm of Eq. (12) is presented as follows:

$$l^{*} \propto (n-d)\log\left(1-\frac{e}{e-1}\left(1-e^{-\left(1-e^{-\lambda\tau^{\delta}}\left(\frac{\lambda\tau^{\delta}(\lambda\tau^{\delta}+2)}{\lambda+2}+1\right)\right)}\right)\right)+d\left(\log\delta+2\log\lambda-\log(\lambda+2)\right)$$

$$+(\delta-1)\sum_{i=1}^{d}\log x_{i:n}-\lambda\sum_{i=1}^{d}x_{i:n}^{\delta}+\sum_{i=1}^{d}\log\left(\lambda x_{i:n}^{2\delta}+1\right)-\sum_{i=1}^{d}\left(1-e^{-\lambda x_{i:n}^{\delta}}\left(\frac{\lambda x_{i:n}^{\delta}(\lambda x_{i:n}^{\delta}+2)}{\lambda+2}+1\right)\right). \tag{13}$$

The maximum likelihood estimators $\hat{\delta}$ and $\hat{\lambda}$ are derived by differentiating Eq. (13) with respect to the parameters δ and λ, respectively, and setting the resulting expressions to zero.

$$\frac{\partial l^{*}}{\partial\delta}=(n-d)\frac{\frac{e}{e-1}A^{*}(\delta,\lambda,\tau)e^{-\left(1-e^{-\lambda\tau^{\delta}}\left(\frac{\lambda\tau^{\delta}(\lambda\tau^{\delta}+2)}{\lambda+2}+1\right)\right)}}{1-\frac{e}{e-1}\left(1-e^{-\left(1-e^{-\lambda\tau^{\delta}}\left(\frac{\lambda\tau^{\delta}(\lambda\tau^{\delta}+2)}{\lambda+2}+1\right)\right)}\right)}+\frac{d}{\delta}+\sum_{i=1}^{d}\log x_{i:n}-\lambda\sum_{i=1}^{d}x_{i:n}^{\delta}\log x_{i:n}$$

$$+2\lambda\sum_{i=1}^{d}\frac{x_{i:n}^{2\delta}\log x_{i:n}}{\lambda x_{i:n}^{2\delta}+1}+\sum_{i=1}^{d}A^{*}(\delta,\lambda,x_{i:n}), \tag{14}$$

and

$$\frac{\partial l^{*}}{\partial\lambda}=(n-d)\frac{e}{e-1}\frac{B^{*}(\delta,\lambda,\tau)e^{-\left(1-e^{-\lambda\tau^{\delta}}\left(\frac{\lambda\tau^{\delta}(\lambda\tau^{\delta}+2)}{\lambda+2}+1\right)\right)}}{1-\frac{e}{e-1}\left(1-e^{-\left(1-e^{-\lambda\tau^{\delta}}\left(\frac{\lambda\tau^{\delta}(\lambda\tau^{\delta}+2)}{\lambda+2}+1\right)\right)}\right)}+\frac{2d}{\lambda}-\frac{d}{\lambda+2}-\sum_{i=1}^{d}x_{i:n}^{\delta}$$

$$+\lambda\sum_{i=1}^{d}\frac{x_{i:n}^{2\delta}}{\lambda x_{i:n}^{2\delta}+1}+\sum_{i=1}^{d}B^{*}(\delta,\lambda,x_{i:n}),$$

where $A^{*}(\delta,\lambda,x)=\frac{\partial}{\partial\delta}\left(e^{-\lambda x^{\delta}}\left(\frac{\lambda x^{\delta}(\lambda x^{\delta}+2)}{\lambda+2}+1\right)\right)$, and $B^{*}(\delta,\lambda,x)=\frac{\partial}{\partial\lambda}\left(e^{-\lambda x^{\delta}}\left(\frac{\lambda x^{\delta}(\lambda x^{\delta}+2)}{\lambda+2}+1\right)\right)$.

The R'maxLik' package is a robust and efficient instrument for calculating the maximum likelihood estimates $\hat{\delta}$ and $\hat{\lambda}$ via the Newton-Raphson method. This program is frequently employed in statistical analysis as it streamlines the ML estimation procedure.

Moreover, the maximum likelihood estimators (MLEs) of SF and HRF, denoted as $\hat{S}$ and $\hat{H}$, are derived from the aforementioned invariance property:

$$\hat{S}=1-\frac{e}{e-1}\left(1-e^{-\left(1-e^{-\hat{\lambda}x^{\hat{\delta}}}\left(\frac{\hat{\lambda}x^{\hat{\delta}}(\hat{\lambda}x^{\hat{\delta}}+2)}{\hat{\lambda}+2}+1\right)\right)}\right),$$

and

$$\hat{H}=\frac{\frac{e}{e-1}\left(\frac{\hat{\delta}\hat{\lambda}^{2}x^{\hat{\delta}-1}e^{-\hat{\lambda}x^{\hat{\delta}}}(\lambda x^{2\hat{\delta}}+1)}{\lambda+2}\right)e^{-\left(1-e^{-\hat{\lambda}x^{\hat{\delta}}}\left(\frac{\hat{\lambda}x^{\hat{\delta}}(\hat{\lambda}x^{\hat{\delta}}+2)}{\hat{\lambda}+2}+1\right)\right)}}{1-\frac{e}{e-1}\left(1-e^{-\left(1-e^{-\hat{\lambda}x^{\hat{\delta}}}\left(\frac{\hat{\lambda}x^{\hat{\delta}}(\hat{\lambda}x^{\hat{\delta}}+2)}{\hat{\lambda}+2}+1\right)\right)}\right)}.$$

The ACI of the parameters δ and λ is constructed using the asymptotic distribution of the maximum likelihood estimators $\hat{\delta}$ and $\hat{\lambda}$. Acquiring the Fisher information matrix (FIM) is challenging; hence, its observed value is utilized.

$I(\Omega) = I_{i_1,i_2} = \left[\partial^2 l^*(\Omega)/(\partial\Omega_{i_1}\partial\Omega_{i_2})\right], i_1, i_2 = 1, 2, \Omega = (\delta, \lambda)$, and $I^{-1}(\Omega)$ is the inverse of FIM.

Thus, the $(1-\varepsilon)\%$ ACIs for $\Omega = (\delta, \lambda)$, are given by $\hat{\Omega} \pm Z_{\varepsilon/2}\sqrt{\widehat{\text{var}}(\hat{\Omega})}$, where $Z_{\varepsilon/2}$ denoted the upper $(\varepsilon/2)$ percent point of standard normal distribution, where $Z_{\varepsilon/2}$ is the upper $\varepsilon/2$ quantile of $N(0,1)$.

To construct ACIs for the SF and HRF, we need to estimate their variances. The delta method, as described by Greene [23], provides an approximation for these variances. The approximate variances of $\hat{S}$ and $\hat{H}$ are calculated as follows:

$\text{var}(\hat{S}) = [\Delta\,\hat{S}]^T[I^{-1}(\Omega)][\Delta\hat{S}]$, and $\text{var}(\hat{H}) = [\Delta\hat{H}]^T[I^{-1}(\Omega)][\Delta\hat{H}]$,

where $\Delta\,\hat{S} = \left(\dfrac{\partial R}{\partial\delta}, \dfrac{\partial R}{\partial\lambda}\right)$, and $\Delta\hat{H} = \left(\dfrac{\partial H}{\partial\delta}, \dfrac{\partial H}{\partial\lambda}\right)$.

Thus, the two-sided $100(1-\varepsilon)\%$ ACI of $\hat{S}$ and $\hat{H}$ can be constructed as follows:

$\hat{S} \pm Z_{\varepsilon/2}\sqrt{\widehat{\text{var}}(\hat{S})}, \quad \hat{H} \pm Z_{\varepsilon/2}\sqrt{\widehat{\text{var}}(\hat{H})}$.

5.3 Maximum Product Spacing Method

In certain circumstances, the MPS strategy has numerous advantages over conventional ML methods, making it a formidable alternative. The study by [24,25] provides substantial insights into the consistency and asymptotic properties of MPS estimators (MPSEs). Their research indicates that MPSEs can offer equivalent or superior efficiency to MLEs, rendering them a viable alternative.

Let $x_{(1)}, x_{(2)}, \ldots, x_{(n)}$ denote an ordered random sample of size n drawn from the KMPCJD. The uniform spacings are characterized as the differences:

$$D_i(\Omega) = F\left(x_{(i)}; \Omega\right) - F\left(x_{(i-1)}; \Omega\right), \quad i = 1, 2, \ldots, n+1,$$

where $F\left(x_{(0)}; \Omega\right) = 0, F\left(x_{(n+1)}; \Omega\right) = 1$, such that $\sum_{i=1}^{n+1} D_i(\Omega) = 1$.

The general MPS expression for hybrid censored samples is as follows:

$$l_1(\Omega) \propto [1 - F(\tau; \Omega)]^{n-d} \prod_{i=1}^{d+1} [D_i(\Omega)].$$

The MPSEs of the KMPCJD parameters derived from hybrid censored samples are achieved by optimizing the following function:

$$\ln l_1(\Omega) = \left[1 - \frac{e}{e-1}\left(1 - e^{-\left(1-e^{-\lambda\tau^\delta}\left(\frac{\lambda\tau^\delta(\lambda\tau^\delta+2)}{\lambda+2}+1\right)\right)}\right)\right]^{n-d} \prod_{i=1}^{d} \left[\frac{e}{e-1}\left(1 - e^{-\left(1-e^{-\lambda x_{i:n}^\delta}\left(\frac{\lambda x_{i:n}^\delta(\lambda x_{i:n}^\delta+2)}{\lambda+2}+1\right)\right)}\right)\right.$$
$$\left. - \frac{e}{e-1}\left(1 - e^{-\left(1-e^{-\lambda x_{i-1:n}^\delta}\left(\frac{\lambda x_{i-1:n}^\delta(\lambda x_{i-1:n}^\delta+2)}{\lambda+2}+1\right)\right)}\right)\right]. \tag{15}$$

The MPSE $\hat{\delta}$, and $\hat{\lambda}_1$ of the KMPCJD parameters can be derived by resolving the nonlinear equations concerning δ and λ rather than employing Eq. (15).

The MPSE $\hat{S}$ and $\hat{H}$ are derived from the aforementioned invariance property:

$$\hat{S} = 1 - \frac{e}{e-1}\left(1 - e^{-\left(1-e^{-\hat{\lambda}x^{\hat{\delta}}}\left(\frac{\hat{\lambda}x^{\hat{\delta}}(\hat{\lambda}x^{\hat{\delta}}+2)}{\hat{\lambda}+2}+1\right)\right)}\right),$$

and

$$\hat{H} = \frac{\frac{e}{e-1}\left(\frac{\hat{\delta}\hat{\lambda}^2x^{\hat{\delta}-1}e^{-\hat{\lambda}x^{\hat{\delta}}}(\lambda x^{2\delta}+1)}{\lambda+2}\right)e^{-\left(1-e^{-\hat{\lambda}x^{\hat{\delta}}}\left(\frac{\hat{\lambda}x^{\hat{\delta}}(\hat{\lambda}x^{\hat{\delta}}+2)}{\hat{\lambda}+2}+1\right)\right)}}{1-\frac{e}{e-1}\left(1 - e^{-\left(1-e^{-\hat{\lambda}x^{\hat{\delta}}}\left(\frac{\hat{\lambda}x^{\hat{\delta}}(\hat{\lambda}x^{\hat{\delta}}+2)}{\hat{\lambda}+2}+1\right)\right)}\right)}.$$

Moreover, the MPS methodology is employed to produce the ACIs for the parameters δ, λ, SF, and HRF. This technique parallels that described in the previous subsection, with the MLEs substituted by the MPSEs.

5.4 Bayesian Estimation Method

This study examines the boundary estimates for the KMPCJD parameters, R and H, under hybrid censoring. Assuming that the parameters δ and λ of the KMPCJD possess independent gamma prior distributions. If $\delta \sim \text{Gamma}(c_1, d_1)$, and $\lambda \sim \text{Gamma}(c_2, d_2)$, then the joint prior of δ and λ is as follows:

$$\text{A}(\Omega) \propto \delta^{c_1-1}\lambda^{c_2-1}e^{-(d_1\delta+d_2\lambda)}, \tag{16}$$

where c_i and d_i, for $i = 1, 2$, are the hyperparameters. By integrating the joint prior presented in Eq. (16) with the likelihood function outlined in Eq. (12), we can construct the joint posterior density function.

$$l\left(\Omega\middle|\underline{\mathbf{x}}\right) \propto \left(1 - \frac{e}{e-1}\left(1 - e^{-\left(1-e^{-\lambda\tau^{\delta}}\left(\frac{\lambda\tau^{\delta}(\lambda\tau^{\delta}+2)}{\lambda+2}+1\right)\right)}\right)\right)^{n-d}\prod_{i=1}^{d}\left(\frac{\delta\lambda^2x_{i:n}^{\delta-1}e^{-\lambda x_{i:n}^{\delta}}(\lambda x_{i:n}^{2\delta}+1)}{\lambda+2}\right)$$
$$\times\, \delta^{c_1-1}\lambda^{c_2-1}e^{-(d_1\delta+d_2\lambda)}\left(\frac{e}{e-1}\right)^{d}e^{-\sum_{i=1}^{d}\left(1-e^{-\lambda x_{i:n}^{\delta}}\left(\frac{\lambda x_{i:n}^{\delta}(\lambda x_{i:n}^{\delta}+2)}{\lambda+2}+1\right)\right)}.$$

The marginal posterior densities of δ, λ, SF, and HRF are presented as follows:

$$l\left(\delta\middle|\lambda,\underline{\mathbf{x}}\right) \propto \left(1 - \frac{e}{e-1}\left(1 - e^{-\left(1-e^{-\lambda\tau^{\delta}}\left(\frac{\lambda\tau^{\delta}(\lambda\tau^{\delta}+2)}{\lambda+2}+1\right)\right)}\right)\right)^{n-d}\prod_{i=1}^{d}\left(\delta x_{i:n}^{\delta-1}e^{-\lambda x_{i:n}^{\delta}}(\lambda x_{i:n}^{2\delta}+1)\right)$$
$$\times\, \delta^{c_1-1}e^{-(d_1\delta)}e^{-\sum_{i=1}^{d}\left(1-e^{-\lambda x_{i:n}^{\delta}}\left(\frac{\lambda x_{i:n}^{\delta}(\lambda x_{i:n}^{\delta}+2)}{\lambda+2}+1\right)\right)}, \tag{17}$$

and

$$l\left(\lambda\middle|\delta,\underline{\mathbf{x}}\right)\propto\left(1-\frac{e}{e-1}\left(1-e^{-\left(1-e^{-\lambda\tau^{\delta}}\left(\frac{\lambda\tau^{\delta}(\lambda\tau^{\delta}+2)}{\lambda+2}+1\right)\right)}\right)\right)^{n-d}\prod_{i=1}^{d}\left(\frac{\lambda^{2}e^{-\lambda x_{i:n}^{\delta}}(\lambda x_{i:n}^{2\delta}+1)}{\lambda+2}\right)$$
$$\times\lambda^{c_2-1}e^{-d_2\lambda}e^{-\sum_{i=1}^{d}\left(1-e^{-\lambda x_{i:n}^{\delta}}\left(\frac{\lambda x_{i:n}^{\delta}(\lambda x_{i:n}^{\delta}+2)}{\lambda+2}+1\right)\right)} \tag{18}$$

$$\tilde{R}=1-\frac{e}{e-1}\left(1-e^{-\left(1-e^{-\tilde{\lambda}x^{\tilde{\delta}}}\left(\frac{\tilde{\lambda}x^{\tilde{\delta}}(\tilde{\lambda}x^{\tilde{\delta}}+2)}{\tilde{\lambda}+2}+1\right)\right)}\right), \tag{19}$$

and

$$\tilde{H}=\frac{\frac{e}{e-1}\left(\frac{\tilde{\delta}\tilde{\lambda}^{2}x^{\tilde{\delta}-1}e^{-\tilde{\lambda}x^{\tilde{\delta}}}(\lambda x^{2\tilde{\delta}}+1)}{\lambda+2}\right)e^{-\left(1-e^{-\tilde{\lambda}x^{\tilde{\delta}}}\left(\frac{\tilde{\lambda}x^{\tilde{\delta}}(\tilde{\lambda}x^{\tilde{\delta}}+2)}{\tilde{\lambda}+2}+1\right)\right)}}{1-\frac{e}{e-1}\left(1-e^{-\left(1-e^{-\tilde{\lambda}x^{\tilde{\delta}}}\left(\frac{\tilde{\lambda}x^{\tilde{\delta}}(\tilde{\lambda}x^{\tilde{\delta}}+2)}{\tilde{\lambda}+2}+1\right)\right)}\right)}. \tag{20}$$

Due to the absence of closed-form expressions for the marginal posterior densities in Eqs. (17)–(20), we will generate samples for δ, λ, SF, and HRF utilizing the Metropolis-Hastings (M-H) algorithm with a normal proposal distribution.

The M-H algorithm is a Markov Chain Monte Carlo (MCMC) technique employed to produce samples from a probability distribution, particularly when direct sampling poses challenges. The algorithm operates in the following manner:

- **Initialization:**
  - Choose a starting point for the Markov chain.
  - Specify the target distribution $l\left(\Omega\middle|\underline{\mathbf{t}}\right)$ that we aim to sample from.
  - Determine the total number of iterations I, and set the standard deviation σ_Ω for the normal proposal distribution, typically derived from the Hessian matrix.
- **Repeat for I iterations:**
  - Propose a new candidate value using a normal distribution centered around the current state:

    $\Omega\sim\mathcal{N}(\hat{\Omega},\sigma_\Omega^2)$
  - Calculate the acceptance probability R as:

    $$R=\min\left(1,\frac{l\left(\Omega^{(i)}\middle|\underline{\mathbf{t}}\right)}{l\left(\Omega^{(i-1)}\middle|\underline{\mathbf{t}}\right)}\right).$$
  - Draw a random sample u from the uniform distribution $U(0,1)$.
  - If $u\le R$, accept the proposed value and update the state: $\Omega^{(i+1)}=\Omega^{(i)}$.
  - If not, keep the current state unchanged: $\Omega^{(i+1)}=\Omega^{(i)}$.
- **Final step:** Once all iterations are complete, the sequence of samples approximates the desired target distribution.

6 Simulation Study

This section reports a structured simulation study designed to assess the finite-sample performance of the three estimation procedures introduced (MLE, MPS and Bayesian MCMC) under hybrid censoring. We describe the design, the data-generation mechanism, implementation details, the performance measures, and the way results should be interpreted and linked to the proposed method.

The simulation study pursues three objectives:

1. Quantify bias, mean square error (MSE) and interval lengths for point and interval estimators of the parameters δ and λ and of the derived functions (survival $S(\cdot)$ and hazard $H(\cdot)$).
2. Compare the three estimation strategies (MLE, MPS, Bayesian) across realistic hybrid censoring regimes and sample sizes to evaluate efficiency and robustness.
3. Demonstrate convergence diagnostics and computational cost to inform practical implementation.

For each simulation scenario we generate hybrid-censored samples from the KMPCJD with specified true parameters (δ_0, λ_0) as follows:

1. Fix the sample size n and desired number of failures r and quantile Q (used to determine the censoring time T via the baseline CDF quantile: $T = F^{-1}(Q; \delta_0, \lambda_0)$).
2. Generate n independent lifetimes $X_1, \ldots, X_n$ from the KMPCJD using inverse transform sampling.
3. Order the lifetimes $X_{(1)} \leq \cdots \leq X_{(n)}$ and apply hybrid censoring: observe $d = \min\{r, \#\{X_i \leq T\}\}$ failures and record $\tau = \min\{T, X_{(r)}\}$; the observed sample is $\{X_{(1)}, \ldots, X_{(d)}\}$ and the likelihood is formed as in Eq. (11).
4. Repeat the above to obtain M replicate hybrid-censored datasets per scenario.

Parameter sets were chosen to produce a variety of hazard shapes (increasing, decreasing, J-shaped) and to reflect small and moderate sample sizes encountered in reliability and disability studies. The main scenarios reported in the paper are:

$(\delta, \lambda) \in \{(0.8, 1.3), (0.8, 2.4), (3.0, 2.4), (1.5, 0.4)\}$,

with $n \in \{40, 100, 150\}$ and for each n we consider multiple r values (e.g., $r \in \{0.7n, 0.85n, n\}$) and quantiles $Q \in \{0.5, 0.7, 0.9\}$. The censoring time T was set as $T = F^{-1}(Q; \delta, \lambda)$. Values shown for $Q = 0.5, 0.7, 0.9$ are the corresponding numeric T-values for the parameter sets. These choices intentionally cover low-to-high censoring proportions and produce differing amounts of failure information so we can assess sensitivity of estimators to censoring. The parameter choices are therefore motivated by (i) exploring different HRF shapes and (ii) testing estimator stability across censoring intensities. A brief justification of each chosen combination is given in the manuscript prior to tables presenting results.

For each simulated dataset we compute:

- **MLE:** Numerical maximization of the hybrid censored log-likelihood (Eq. (13)) using a Newton-Raphson optimizer (R package `maxLik`).
- **MPS:** Maximization of the log-product-spacing objective for censored samples (Eq. (15)) using the same numerical optimizer (starting values set to MLE or method-of-moments when available).
- **Bayesian:** Metropolis–Hastings MCMC targeting the joint posterior (Eqs. (17)–(18)) with independent Gamma priors for δ, λ, as described in Section 5.4.

The fundamental difference between MLE, and Bayesian approaches are that parameters are considered random variables with prior distributions. The gamma distribution was utilized as the prior, incorporating shape and scale factors (hyper-parameters). Dey et al. [26] delineated the method of hyper-parameter elicitation, which entailed the selection of these parameters grounded in the features of gamma distribution and ML information.

By equating $\hat{\delta}$ and $\hat{\lambda}$ to the mean and variance of the gamma prior distribution, we may ascertain their respective means and variances. This results in:

$$\frac{1}{I}\sum_{j=1}^{I}\hat{\delta}^j = c_1 d_1 \quad \& \quad \frac{1}{I-1}\sum_{j=1}^{I}\left(\hat{\delta}^j - \frac{1}{I}\sum_{j=1}^{I}\hat{\delta}^j\right)^2 = c_1^2 d_1,$$

$$\frac{1}{I}\sum_{j=1}^{I}\hat{\lambda}^j = c_2 d_2 \quad \& \quad \frac{1}{I-1}\sum_{j=1}^{I}\left(\hat{\lambda}^j - \frac{1}{I}\sum_{j=1}^{I}\hat{\lambda}^j\right)^2 = c_2^2 d_2,$$

where I denotes the total iterations of the MCMC simulation. Upon resolving the aforementioned two equations for each hyper-parameter, the estimated hyper-parameters can be expressed as:

$$c_1 = \frac{\left(\frac{1}{I}\sum_{j=1}^{I}\hat{\delta}^j\right)^2}{\frac{1}{I-1}\sum_{j=1}^{I}\left(\hat{\delta}^j - \frac{1}{I}\sum_{j=1}^{I}\hat{\delta}^j\right)^2} \quad \& \quad d_1 = \frac{\frac{1}{I-1}\sum_{j=1}^{I}\left(\hat{\delta}^j - \frac{1}{I}\sum_{j=1}^{I}\hat{\delta}^j\right)^2}{\frac{1}{I}\sum_{j=1}^{I}\hat{\delta}^j}, \tag{21}$$

$$c_2 = \frac{\left(\frac{1}{I}\sum_{j=1}^{I}\hat{\lambda}^j\right)^2}{\frac{1}{I-1}\sum_{j=1}^{I}\left(\hat{\lambda}^j - \frac{1}{I}\sum_{j=1}^{I}\hat{\lambda}^j\right)^2} \quad \& \quad d_2 = \frac{\frac{1}{I-1}\sum_{j=1}^{I}\left(\hat{\lambda}^j - \frac{1}{I}\sum_{j=1}^{I}\hat{\lambda}^j\right)^2}{\frac{1}{I}\sum_{j=1}^{I}\hat{\lambda}^j}. \tag{22}$$

These estimates are then transformed to obtain $\widehat{S}(\cdot)$ and $\widehat{H}(\cdot)$ using the invariance property. This direct mapping connects the parameter estimators to the primary practical quantities of interest (survival and hazard) and therefore directly links the simulation outcomes to the proposed applied method.

All simulation experiments were performed in R. Key implementation settings:

- Random number seed: `set.seed(20250911)` for all Monte Carlo replications and `set.seed(20250911)` before any real-data analyses to ensure reproducibility. (Change the seed only if re-running a new batch.)
- Number of Monte Carlo replicates: $M = 5000$ (i.e., 5000 datasets per scenario). This yields stable estimates of Bias and MSE while keeping computational cost moderate.
- MLE/MPS maximization: `maxLik::maxLik(..., method="BFGS")` or Newton–Raphson with tolerance `tol = 1e-8` and `maxit = 1000`; starting values = method-of-moments or small perturbation of true values.
- Bayesian MCMC: Metropolis–Hastings with total iterations $I = 10{,}000$, burn-in $B = 2000$, and thinning $k = 1$ (so posterior sample size ≈ 8000 per chain).
- Software packages cited in the manuscript: `maxLik` [27], `coda` [28], and base `stats`.

For each scenario and estimator we compute the following summaries across the M replicates:

- **Bias** $= \bar{\hat{\theta}} - \theta_0$,

- **MSE** $= \overline{(\hat{\theta} - \theta_0)^2}$,
- **Average interval length** for asymptotic/confidence intervals (LACI) and Bayesian credible intervals (LCCI),
- **Coverage probability** (proportion of replicates where the nominal 95% interval contains θ_0),
- For $S(\cdot)$ and $H(\cdot)$ we report pointwise Bias/MSE at representative time points (e.g., median, 75th quantile).

Tables 1–4 summarize Bias, MSE and interval lengths for δ, λ, S, H. Figures show behavior across r and Q to visualize sensitivity to censoring and sample size.

Table 1: Parameter and reliability analysis using Bayesian, MPS, and MLE estimation methodologies: $\delta = 0.8, \lambda = 1.3$

				MLE			MPS			Bayesian		
n	r	Q		Bias	MSE	LACI	Bias	MSE	LACI	Bias	MSE	LCCI
40	28	0.5	δ	0.0460	0.0333	0.7012	−0.0738	0.0296	0.7291	0.0078	0.0098	0.3853
			λ	−0.0081	0.0333	0.7145	−0.0023	0.0340	0.7158	−0.0020	0.0112	0.4040
			S	0.0057	0.0055	0.2918	0.0278	0.0055	0.2728	0.0040	0.0022	0.1809
			H	0.0742	0.0260	0.6203	−0.0906	0.0208	0.6152	0.0079	0.0091	0.3686
	35	0.7	δ	0.0275	0.0177	0.5147	−0.0569	0.0174	0.5526	0.0010	0.0056	0.2847
			λ	−0.0025	0.0327	0.7095	0.0021	0.0307	0.6491	−0.0006	0.0070	0.3261
			S	−0.0050	0.0049	0.2745	0.0251	0.0050	0.2530	0.0039	0.0020	0.1765
			H	0.0708	0.0238	0.5905	−0.0727	0.0186	0.5857	0.0062	0.0091	0.3579
	40	0.9	δ	0.0269	0.0117	0.4142	−0.0394	0.0110	0.4461	−0.0006	0.0026	0.1994
			λ	−0.0023	0.0319	0.7003	0.0020	0.0307	0.6399	−0.0002	0.0035	0.2281
			S	−0.0041	0.0017	0.1631	0.0151	0.0021	0.1528	0.0030	0.0009	0.1114
			H	0.0595	0.0219	0.5640	−0.0566	0.0169	0.5612	0.0050	0.0084	0.3493
100	75	0.5	δ	0.0232	0.0126	0.4333	−0.0329	0.0119	0.4593	0.0064	0.0057	0.2848
			λ	−0.0049	0.0151	0.4816	0.0022	0.0146	0.4677	−0.0012	0.0062	0.3031
			S	−0.0043	0.0026	0.2004	0.0083	0.0026	0.1926	0.0005	0.0013	0.1331
			H	0.0424	0.0104	0.3939	−0.0346	0.0092	0.4043	0.0061	0.0056	0.2832
	85	0.7	δ	0.0123	0.0071	0.3277	−0.0266	0.0071	0.3507	0.0009	0.0028	0.2085
			λ	−0.0025	0.0128	0.4431	0.0019	0.0124	0.4198	−0.0005	0.0050	0.2656
			S	−0.0036	0.0020	0.1751	0.0072	0.0020	0.1662	0.0004	0.0011	0.1138
			H	0.0289	0.0089	0.3657	−0.0336	0.0080	0.3757	0.0049	0.0053	0.2815
	100	0.9	δ	0.0078	0.0042	0.2533	−0.0233	0.0043	0.2719	0.0003	0.0016	0.1545
			λ	0.0022	0.0123	0.4446	0.0016	0.0113	0.4204	0.0001	0.0027	0.2004
			S	−0.0032	0.0007	0.1016	0.0061	0.0007	0.0958	0.0003	0.0005	0.0816
			H	0.0211	0.0086	0.3581	−0.0315	0.0074	0.3646	0.0047	0.0048	0.2598
150	110	0.5	δ	0.0112	0.0075	0.3386	−0.0286	0.0075	0.3584	0.0032	0.0032	0.2127
			λ	0.0028	0.0103	0.3971	0.0018	0.0100	0.3876	0.0011	0.0047	0.2654
			S	−0.0041	0.0017	0.1602	0.0038	0.0016	0.1551	−0.0003	0.0009	0.1145
			H	0.0250	0.0058	0.2969	−0.0294	0.0054	0.3081	0.0051	0.0031	0.2140

(Continued)

Table 1 (continued)

n	r	Q		MLE Bias	MLE MSE	MLE LACI	MPS Bias	MPS MSE	MPS LACI	Bayesian Bias	Bayesian MSE	Bayesian LCCI
	130	0.7	δ	0.0057	0.0045	0.2636	−0.0219	0.0047	0.2806	0.0007	0.0019	0.1700
			λ	−0.0023	0.0089	0.3698	0.0016	0.0087	0.3538	−0.0002	0.0038	0.2368
			S	0.0035	0.0013	0.1427	0.0022	0.0014	0.1367	0.0003	0.0009	0.1120
			H	0.0118	0.0054	0.2879	−0.0338	0.0052	0.2977	0.0045	0.0034	0.2187
	150	0.9	δ	0.0061	0.0027	0.2023	−0.0117	0.0027	0.2167	0.0002	0.0011	0.1303
			λ	−0.0020	0.0091	0.3730	0.0015	0.0090	0.3572	−0.0001	0.0025	0.1926
			S	−0.0026	0.0005	0.0842	0.0046	0.0005	0.0799	0.0002	0.0003	0.0692
			H	0.0207	0.0053	0.2811	−0.0197	0.0047	0.2899	0.0039	0.0034	0.2235

Table 2: Parameter and reliability analysis using Bayesian, MPS, and MLE estimation methodologies: $\delta = 0.8, \lambda = 2.4$

n	r	Q		MLE Bias	MLE MSE	MLE LACI	MPS Bias	MPS MSE	MPS LACI	Bayesian Bias	Bayesian MSE	Bayesian LCCI
40	28	0.5	δ	0.0407	0.0357	0.7305	−0.0778	0.0319	0.7510	−0.0072	0.0090	0.3603
			λ	0.0327	0.2486	1.9312	−0.0351	0.2113	1.9352	−0.0022	0.0175	0.5203
			S	−0.0252	0.0067	0.3221	0.0224	0.0066	0.3020	0.0042	0.0011	0.1216
			H	0.0672	0.1468	1.4775	−0.0782	0.1195	1.4688	−0.0082	0.0102	0.4024
	35	0.7	δ	0.0275	0.0204	0.5541	−0.0623	0.0196	0.5851	−0.0019	0.0061	0.3053
			λ	0.0156	0.1433	1.4776	−0.0165	0.1261	1.4609	−0.0014	0.0094	0.3728
			S	−0.0028	0.0052	0.2839	0.0205	0.0053	0.2634	0.0015	0.0004	0.0820
			H	0.0609	0.1321	1.3970	−0.0701	0.1018	1.3634	−0.0053	0.0105	0.3708
	40	0.9	δ	0.0253	0.0145	0.4627	−0.0447	0.0133	0.4907	−0.0016	0.0030	0.2121
			λ	0.0114	0.0849	1.1381	−0.0049	0.0713	1.0853	−0.0013	0.0037	0.2375
			S	−0.0024	0.0018	0.1678	0.0192	0.0022	0.1571	0.0015	0.0002	0.0542
			H	0.0596	0.1305	1.2483	−0.0633	0.1021	1.2978	−0.0011	0.0109	0.3538
100	75	0.5	δ	0.0220	0.0128	0.4383	−0.0342	0.0122	0.4646	0.0061	0.0049	0.2728
			λ	0.0147	0.0878	1.1541	−0.0167	0.0820	1.1874	−0.0013	0.0143	0.4648
			S	−0.0093	0.0025	0.1957	0.0104	0.0025	0.1881	0.0040	0.0007	0.1058
			H	0.0319	0.0522	0.8867	−0.0363	0.0478	0.9154	−0.0011	0.0080	0.3482
	85	0.7	δ	0.0105	0.0073	0.3335	−0.0315	0.0074	0.3565	−0.0016	0.0033	0.2221
			λ	0.0065	0.0462	0.8410	−0.0075	0.0439	0.8519	−0.0012	0.0082	0.3500
			S	−0.0016	0.0021	0.1795	0.0103	0.0021	0.1710	0.0014	0.0004	0.0766
			H	0.0257	0.0420	0.7968	−0.0351	0.0384	0.8189	−0.0010	0.0080	0.3082
	100	0.9	δ	0.0088	0.0050	0.2755	−0.0255	0.0051	0.2944	−0.0012	0.0019	0.1698
			λ	0.0020	0.0316	0.6969	−0.0043	0.0294	0.6868	−0.0005	0.0034	0.2258
			S	0.0014	0.0007	0.1058	0.0086	0.0008	0.1000	0.0010	0.0001	0.0475
			H	0.0246	0.0403	0.6809	−0.0104	0.0383	0.8213	−0.0009	0.0070	0.2943

(Continued)

Table 2 (continued)

				MLE			MPS			Bayesian		
n	r	Q		Bias	MSE	LACI	Bias	MSE	LACI	Bias	MSE	LCCI
150	110	0.5	δ	0.0139	0.0079	0.3455	−0.0258	0.0077	0.3657	0.0061	0.0034	0.2216
			λ	0.0076	0.0537	0.9059	−0.0143	0.0519	0.9357	−0.0007	0.0132	0.4468
			S	0.0009	0.0016	0.1574	0.0088	0.0016	0.1524	0.0038	0.0006	0.0947
			H	0.0177	0.0313	0.6903	−0.0302	0.0299	0.7166	0.0008	0.0069	0.3150
	130	0.7	δ	0.0102	0.0056	0.2923	−0.0176	0.0055	0.3097	0.0014	0.0025	0.1904
			λ	0.0062	0.0298	0.6743	−0.0035	0.0286	0.6851	0.0006	0.0074	0.3299
			S	−0.0008	0.0014	0.1460	0.0070	0.0014	0.1402	−0.0006	0.0003	0.0721
			H	0.0153	0.0306	0.6777	−0.0187	0.0280	0.6982	0.0006	0.0058	0.2551
	150	0.9	δ	0.0064	0.0037	0.2373	−0.0176	0.0037	0.2516	0.0007	0.0014	0.1427
			λ	0.0016	0.0213	0.5692	0.0019	0.0200	0.5649	−0.0004	0.0034	0.2258
			S	−0.0006	0.0005	0.0867	0.0064	0.0005	0.0825	0.0004	0.0001	0.0419
			H	0.0121	0.0283	0.6853	−0.0092	0.0279	0.7009	0.0005	0.0057	0.2772

Table 3: Parameter and reliability analysis using Bayesian, MPS, and MLE estimation methodologies: $\delta = 3, \lambda = 2.4$

				MLE			MPS			Bayesian		
n	r	Q		Bias	MSE	LACI	Bias	MSE	LACI	Bias	MSE	LCCI
40	28	0.5	δ	0.0648	0.5516	2.8111	−0.0562	0.4525	2.9172	−0.0053	0.0191	0.5281
			λ	0.0347	0.3007	2.1258	−0.0374	0.2805	2.2200	0.0014	0.0180	0.5219
			S	0.0072	0.0064	0.3136	0.0527	0.0063	0.2936	−0.0031	0.0008	0.1088
			H	0.0856	0.9530	3.7377	−0.0622	0.7398	3.6843	0.0020	0.0443	0.8011
	35	0.7	δ	0.0390	0.3333	2.2170	−0.0523	0.2991	2.3286	−0.0010	0.0099	0.3763
			λ	0.0172	0.1387	1.4519	−0.0151	0.1220	1.4399	−0.0004	0.0087	0.3585
			S	−0.0066	0.0052	0.2817	0.0492	0.0052	0.2610	0.0027	0.0004	0.0780
			H	0.0854	0.9167	3.2614	−0.0564	0.6184	3.4785	−0.0013	0.0407	0.8006
	40	0.9	δ	0.0265	0.1967	1.7110	−0.0483	0.1863	1.8190	−0.0008	0.0043	0.2600
			λ	0.0098	0.0866	1.1507	−0.0065	0.0728	1.0954	0.0002	0.0038	0.2406
			S	0.0057	0.0018	0.1656	0.0417	0.0022	0.1547	0.0024	0.0001	0.0354
			H	0.0836	0.7784	3.1463	−0.0473	0.5936	2.9612	−0.0005	0.0305	0.7536
100	75	0.5	δ	0.0200	0.1635	1.5683	−0.0361	0.1585	1.6709	−0.0016	0.0163	0.4895
			λ	0.0188	0.0843	1.1246	−0.0138	0.0876	1.2318	0.0005	0.0150	0.4873
			S	−0.0061	0.0025	0.1966	0.0353	0.0025	0.1888	0.0025	0.0007	0.1047
			H	0.0369	0.2739	2.0210	−0.0317	0.2463	2.0914	0.0007	0.0362	0.7366
	85	0.7	δ	0.0121	0.1203	1.3531	−0.0301	0.1189	1.4321	−0.0009	0.0092	0.3673
			λ	0.0070	0.0418	0.7996	−0.0070	0.0396	0.8113	−0.0004	0.0087	0.3600
			S	−0.0036	0.0019	0.1698	0.0215	0.0019	0.1612	0.0023	0.0004	0.0729
			H	0.0282	0.2063	2.0092	−0.0305	0.2057	2.0171	−0.0006	0.0271	0.7090

(Continued)

Table 3 (continued)

n	r	Q		MLE Bias	MLE MSE	MLE LACI	MPS Bias	MPS MSE	MPS LACI	Bayesian Bias	Bayesian MSE	Bayesian LCCI
	100	0.9	δ	0.0106	0.0735	1.0561	−0.0237	0.0730	1.1249	−0.0007	0.0042	0.2502
			λ	0.0045	0.0346	0.7281	−0.0019	0.0320	0.7171	−0.0001	0.0035	0.2357
			S	0.0016	0.0008	0.1079	0.0204	0.0008	0.1020	0.0019	0.0001	0.0330
			H	0.0233	0.1847	1.9252	−0.0306	0.1946	2.0031	−0.0003	0.0231	0.6360
150	110	0.5	δ	0.0185	0.1163	1.3196	−0.0212	0.1098	1.3945	0.0016	0.0154	0.4809
			λ	0.0102	0.0504	0.8752	−0.0119	0.0481	0.9056	0.0002	0.0123	0.4285
			S	−0.0022	0.0015	0.1536	0.0076	0.0015	0.1486	0.0006	0.0005	0.0883
			H	0.0227	0.1669	1.5872	−0.0254	0.1565	1.6508	0.0006	0.0308	0.6633
	130	0.7	δ	0.0122	0.0720	1.0426	−0.0176	0.0700	1.1064	−0.0009	0.0086	0.3650
			λ	0.0055	0.0295	0.6716	−0.0041	0.0283	0.6819	0.0003	0.0075	0.3377
			S	−0.0014	0.0013	0.1439	0.0061	0.0013	0.1380	0.0002	0.0004	0.0731
			H	0.0124	0.1282	1.4840	−0.0209	0.1205	1.4785	−0.0004	0.0161	0.6093
	150	0.9	δ	0.0104	0.0473	0.8440	−0.0137	0.0458	0.8962	0.0003	0.0038	0.2373
			λ	0.0040	0.0209	0.5661	−0.0019	0.0198	0.5619	−0.0001	0.0034	0.2216
			S	−0.0013	0.0005	0.0851	0.0051	0.0005	0.0808	0.0001	0.0001	0.0330
			H	0.0121	0.1057	1.1427	−0.0193	0.1009	1.3912	0.0002	0.0116	0.5299

Table 4: Parameter and reliability analysis using Bayesian, MPS, and MLE estimation methodologies: $\delta = 1.5, \lambda = 0.4$

n	r	Q		MLE Bias	MLE MSE	MLE LACI	MPS Bias	MPS MSE	MPS LACI	Bayesian Bias	Bayesian MSE	Bayesian LCCI
40	28	0.5	δ	0.0100	0.3448	2.3024	−0.0628	0.0691	1.0711	−0.0025	0.0127	0.4401
			λ	−0.1635	1.9739	5.5042	0.1116	0.0138	0.3162	0.0096	0.0030	0.2115
			S	−0.0042	0.0067	0.3204	0.0209	0.0060	0.2898	−0.0013	0.0058	0.2931
			H	0.0628	0.0333	0.7050	−0.0772	0.0279	0.7075	0.0183	0.0178	0.5120
	35	0.7	δ	0.0097	0.1341	1.4352	−0.0440	0.0431	0.8523	−0.0019	0.0065	0.3159
			λ	−0.1404	0.9998	3.9154	0.0961	0.0115	0.2985	0.0091	0.0023	0.1874
			S	−0.0033	0.0057	0.3035	0.0195	0.0052	0.2625	0.0009	0.0045	0.2636
			H	0.0594	0.0314	0.6810	−0.0576	0.0204	0.6804	0.0163	0.0152	0.4780
	40	0.9	δ	0.0092	0.0641	0.9888	−0.0376	0.0337	0.7642	−0.0018	0.0031	0.2253
			λ	−0.0405	0.2165	1.8237	0.0897	0.0102	0.2347	0.0026	0.0015	0.1481
			S	0.0023	0.0027	0.2017	0.0169	0.0022	0.1582	0.0007	0.0017	0.1497
			H	0.0461	0.0308	0.6076	−0.0463	0.0160	0.6048	0.0003	0.0128	0.4633
100	75	0.5	δ	0.0092	0.0256	0.6193	−0.0238	0.0252	0.6689	−0.0009	0.0078	0.3424
			λ	−0.0142	0.0043	0.2551	0.0418	0.0046	0.2368	0.0056	0.0015	0.1484
			S	−0.0029	0.0025	0.1963	0.0083	0.0025	0.1886	−0.0011	0.0023	0.1888
			H	0.0370	0.0123	0.4278	−0.0296	0.0111	0.4436	0.0129	0.0078	0.3484

(Continued)

Table 4 (continued)

n	r	Q		MLE			MPS			Bayesian		
				Bias	MSE	LACI	Bias	MSE	LACI	Bias	MSE	LCCI
	85	0.7	δ	0.0061	0.0173	0.5151	−0.0211	0.0180	0.5519	−0.0001	0.0045	0.2597
			λ	0.0018	0.0041	0.2511	0.0409	0.0047	0.2371	0.0048	0.0012	0.1359
			S	−0.0005	0.0019	0.1710	0.0079	0.0019	0.1627	0.0003	0.0018	0.1681
			H	0.0190	0.0106	0.4087	−0.0235	0.0105	0.4032	0.0042	0.0069	0.3079
	100	0.9	δ	0.0057	0.0118	0.4244	−0.0185	0.0120	0.4538	−0.0001	0.0024	0.1930
			λ	0.0004	0.0037	0.2392	0.0403	0.0042	0.2261	0.0015	0.0009	0.1190
			S	−0.0004	0.0006	0.0996	0.0061	0.0007	0.0945	0.0002	0.0006	0.0922
			H	0.0125	0.0102	0.4060	−0.0210	0.0091	0.3562	0.0003	0.0051	0.3072
150	110	0.5	δ	0.0070	0.0189	0.5372	−0.0221	0.0194	0.5740	−0.0007	0.0059	0.2957
			λ	−0.0029	0.0034	0.2288	0.0369	0.0037	0.2162	0.0048	0.0011	0.1241
			S	0.0011	0.0016	0.1576	0.0088	0.0016	0.1525	−0.0006	0.0014	0.1449
			H	0.0140	0.0077	0.3428	−0.0203	0.0075	0.3563	0.0042	0.0049	0.2663
	130	0.7	δ	0.0057	0.0118	0.4234	−0.0143	0.0119	0.4512	−0.0001	0.0035	0.2242
			λ	−0.0014	0.0028	0.2081	0.0294	0.0030	0.1980	0.0048	0.0008	0.1106
			S	−0.0004	0.0012	0.1373	0.0062	0.0012	0.1317	−0.0003	0.0011	0.1274
			H	0.0120	0.0071	0.3290	−0.0172	0.0070	0.3405	0.0035	0.0026	0.2296
	150	0.9	δ	0.0048	0.0079	0.3469	−0.0131	0.0080	0.3685	−0.0001	0.0020	0.1693
			λ	0.0002	0.0024	0.1925	0.0326	0.0026	0.1829	0.0010	0.0007	0.1036
			S	−0.0003	0.0004	0.0829	0.0054	0.0005	0.0791	0.0003	0.0004	0.0808
			H	0.0104	0.0061	0.3096	−0.0085	0.0071	0.3351	0.0001	0.0022	0.0271

We explicitly report burn-in and convergence diagnostics for the Bayesian chains:

- Burn-in of $B = 2000$ iterations was chosen after exploratory runs showed stabilization of trace plots prior to 2000. The posterior summaries are computed from the remaining $I - B$ samples.
- Convergence checks: $\hat{R} < 1.1$ and ESS > 500 for both parameters are used as acceptance criteria.
- Robustness: we repeat a subset of scenarios with different starting points and with alternative prior hyper-parameters to confirm posterior stability; differences were negligible in the reported scenarios.

A practical account of computational cost:

- **MLE/MPS:** each likelihood (or spacing) evaluation costs $O(d)$ operations where d is observed failures; the optimizer typically requires tens to a few hundred evaluations. Hence roughly $O(\text{iter} \times d)$ arithmetic operations per dataset. On a modern desktop using `maxLik` this corresponds to seconds per replication for $n \leq 150$ (exact time depends on starting values and censoring).
- **Bayesian MCMC:** cost is $O(I \times d)$ per dataset; with $I = 10{,}000$ and $d \leq n$ the wall-clock time is larger than a single MLE fit but remains practical for routine simulation (parallelization across replicates is recommended).

- In the manuscript we report elapsed times for representative scenarios (e.g., average seconds per replication) so readers can assess feasibility for their own datasets.

To make the simulation findings transparent and reproducible, each of Tables 1–4 is accompanied by a short stepwise interpretation in the paper:

1. Recap the scenario (true (δ, λ), n, r, Q).
2. List observed numerical summaries (Bias, MSE, LACI, LCCI).
3. Highlight the practical implications (which estimator gives the smallest MSE and the shortest interval).
4. Explain why the observed pattern matches theoretical expectations (e.g., increased n, r or T leads to improved information and therefore decreased Bias/MSE).
5. Note any anomalies and diagnostics (e.g., occasional non-convergence of the optimizer for poor starting values).

The simulation study demonstrates that:

- All three methods produce consistent estimators, with performance improving as n or observed failures increase.
- The Bayesian estimator tends to produce shorter credible intervals in the scenarios studied, indicating potentially higher finite-sample precision when informative priors or data-driven hyper-parameter choices are used.
- From a practical viewpoint the MLE provides a quick, reliable baseline estimate; MPS offers an alternative when MLE is unstable; Bayesian MCMC gives richer uncertainty summaries at a modest additional cost.

These findings emphasize both practical recommendations for applied analysts and academic contributions: the paper supplies a reproducible comparison of three estimation strategies under hybrid censoring for the new KMPCJD family, documents diagnostic checks and computational considerations, and provides guidance for choosing a method depending on data availability and practitioner priorities.

Based on the results presented in Tables 1–4, the following observations can be made:

- When the sample size n increases while keeping other factors like r and T constant, the estimators for δ and λ show improved performance in terms of reduced Bias, MSE, and narrower confidence intervals.
- An increase in the censored sample size r leads to a reduction in Bias, MSE, and the length of the confidence intervals (LCI), indicating better estimation accuracy.
- Similarly, increasing the censoring time T also results in lower Bias, MSE, and LCI, further supporting improved estimation quality.
- These reductions with larger samples highlight the estimators' consistency and accuracy.
- All three estimation techniques yield satisfactory results for the KMPCJD model parameters.
- Among the methods, the Bayesian approach provides the most accurate estimates.
- The Bayesian method also produces shorter credible intervals (LCCI) compared to the traditional confidence intervals (LACI) from ML and MPS methods, suggesting higher precision.

7 Analysis to Engineering and Disability Data

In this section, we show the effectiveness of the KMPCJD in a data fitting scenario using five real-world datasets related to engineering and disability. Several competing models are compared to the KMPCJD, including Kavya Manoharan Rayleigh Inverted Weibull distribution (KMRIWD) [29], Kavya Manoharan Burr X distribution (KMBXD) [30], exponentiated generalized power Lindley distribution (EGPLD) [31], Weibull power Lindley distribution (WPLD) [32], power Lindley distribution (PLD) [33], KMGED, power XLindley distribution (PXLD), Kavya Manoharan unit exponentiated half logistic distribution (KMUEHLD) [34], and PCJD.

The Kolmogorov-Smirnov (Y_1) statistic, p-value of Y_1 (Y_{1Pv}), the Cramér von Mises statistic (Y_2), p-value of Y_2 (Y_{2Pv}), the Anderson-Darling statistics (Y_3), and p-value of Y_3 (Y_{3Pv}) are among the six well-referenced measures of goodness of fit that we consider when comparing the related models. The model with the highest Y_{1Pv}, Y_{2Pv}, and Y_{3Pv} values and the lowest feasible way of Y_1, Y_2, and Y_3 values.

To give readers, especially non-specialists, a clearer understanding of the empirical datasets, we briefly describe each source. The first engineering dataset represents tensile-strength measurements (in GPa) of individual carbon fibers, a critical property in aerospace, automotive, and sports applications. The second engineering dataset contains daily totals of global UV-B radiation (Wh/m^2) collected at the Solar Radiation Research Laboratory (Golden, CO, USA) during June 2025, including location coordinates and instrument specifications.

For the disability data, three subsets—males, females, and total population—are extracted from the Saudi Disability Survey 2023 (General Authority for Statistics). Variables include type and severity of disability (mobility, vision, hearing, cognitive, and mental-health), age, gender, and region, with lifetime-type measurements expressed as the duration (in years) since onset of disability.

7.1 Application to Engineering Data

In this subsection, we used two real data sets related to engineering science to show the importance and flexibility of the new suggested model.

The first dataset

The dataset, sourced from [35], reports tensile strength measurements (in GPa) for individual carbon fibers:

{1.098, 1.253, 0.944, 1.055, 1.586, 1.773, 1.554, 2.012, 1.301, 1.179, 1.884, 0.966, 0.552, 1.179, 1.642, 0.312, 1.426, 1.726, 0.865, 1.063, 0.803, 1.514, 1.270, 2.233, 1.301, 1.240, 1.627, 2.096, 1.533, 1.534, 1.321, 1.801, 1.559, 0.865, 0.979, 2.094, 1.300, 0.865, 1.434, 1.235, 2.585, 1.684, 2.012, 1.048, 1.373, 1.633, 1.697, 0.753, 1.726, 1.754}.

Tensile strength, expressed in GPa, denotes the maximum stress a single carbon fiber can withstand before fracture. It is a critical property for evaluating the performance of carbon fiber–reinforced composites widely used in aerospace, automotive, and sports industries. This dataset illustrates the variability in tensile strength among fibers, providing valuable insights for optimizing composite design and enhancing durability in demanding applications.

The second dataset

This dataset represents the daily totals of global UV-B radiation on a horizontal surface measured at the *Solar Radiation Research Laboratory (SRRL)* Baseline Measurement System (BMS), Golden, CO, USA, during June 2025. The dataset comprises one observation per calendar day ($n = 30$ days), reported in **Watt-hours per square meter (Wh/m²)** (https://catalog.data.gov/ (accessed on 18 September 2025)) and this data mentioned in Table 5.

Table 5: Daily totals of global UV-B radiation (Wh/m²) at SRRL, June 2025

Day	1	2	3	4	5	6	7	8
Wh/m²	7.54	6.43	2.59	8.91	7.67	6.14	9.33	8.02
Day	9	10	11	12	13	14	15	16
Wh/m²	11.45	10.96	7.94	6.82	9.71	10.95	9.39	9.75
Day	17	18	19	20	21	22	23	24
Wh/m²	3.96	12.10	**12.55**	11.84	11.76	**12.55**	8.01	7.91
Day	25	26	27	28	29	30		
Wh/m²	7.55	10.96	8.83	9.87	7.41	9.44		

Measurements were acquired at SRRL (39.74°N, 105.18°W; 1829 m AMSL; Mountain Time UTC−7), located on South Table Mountain with excellent year-round solar access. The UV-B instrument is the *Solar Light Model 501A* biometer-radiometer (serial no. 1898), a meteorological-grade device for erythemally-weighted UV-B monitoring. Data were retrieved from NREL *Measurement & Instrumentation Data Center (MIDC)* for the SRRL BMS site.

Fig. 4 shows the time series of daily totals with markers at the monthly minimum and maximum. An optional horizontal line at the monthly mean (8.95 Wh/m²) may be included to illustrate deviations from the average.

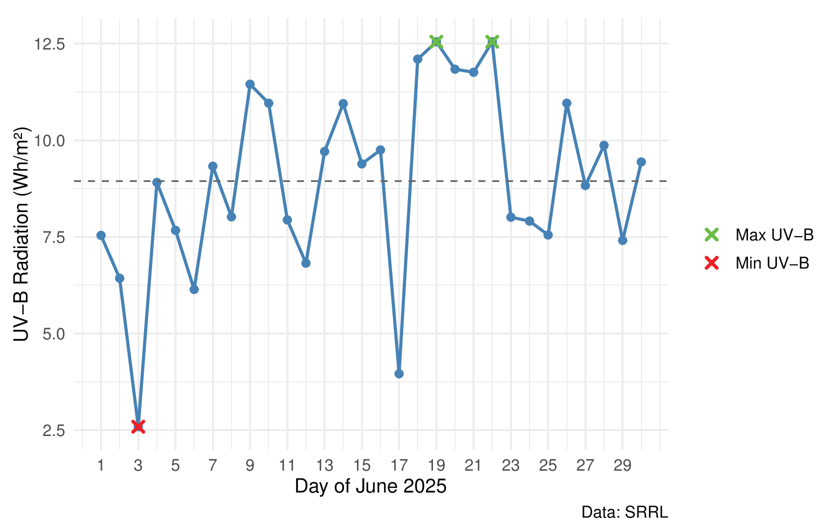

Figure 4: Daily UV-B radiation totals at SRRL (June 2025)

The MLEs and their standard error (SE), as well as the Y_1, Y_{1Pv}, Y_2, Y_{2Pv}, Y_3, and Y_{3Pv} statistics, are shown for the KMPCJD distribution and others in Tables 6 and 7, for both engineering datasets. The histogram, violin plot, quantile-quantile (QQ) plot, box plot with stripchart, and total time on test (TTT) plots, countour plots of log-likelihood values with KMPCJD parameters are shown in

Figs. 5–7 for both engineering datasets. Figs. 8 and 11 show the estimated PDFs, and Figs. 9 and 12 show the estimated CDFs of the competing models for both engineering datasets. Figs. 10 and 13 also show the probability-probability (PP) plots of the competing models for both engineering datasets.

Table 6: The Y_1, Y_{1Pv}, Y_2, Y_{2Pv}, Y_3, Y_{3Pv}, MLEs, and SEs for carbon fibers dataset

Name	Y_1 Y_{1Pv}	Y_2 Y_{2Pv}	Y_3 Y_{3Pv}	$\hat{\delta}$ $SE(\hat{\delta})$	$\hat{\lambda}$ $SE(\hat{\lambda})$	$\hat{\theta}$ $SE(\hat{\theta})$	$\hat{\beta}$ $SE(\hat{\beta})$
KMPCJD	0.0484 (0.9970)	0.0196 (0.9976)	0.1776 (0.9954)	0.6168 (0.0808)	2.6496 (0.2093)		
PCJD	0.0521 (0.9921)	0.0243 (0.9915)	0.2100 (0.9875)	2.4717 (0.2014)	0.8038 (0.1038)		
KMRIWD	0.2030 (0.0068)	0.8326 (0.0060)	5.1606 (0.0025)	0.7985 (0.0637)	1.2433 (0.0675)		
KMBXD	0.0794 (0.7773)	0.0982 (0.5953)	0.6855 (0.5705)	2.3032 (0.3809)	0.7429 (0.0521)		
KMLoLD	0.0719 (0.8680)	0.0664 (0.7758)	0.7489 (0.5189)	4.5721 (0.4671)	1.5745 (0.0708)		
KMGED	0.1071 (0.4070)	0.2220 (0.2289)	1.5834 (0.1579)	8.4118 (1.8169)	1.6227 (0.1738)		
EGPLD	0.0492 (0.9896)	0.0207 (0.9889)	0.1853 (0.9872)	2.8135 (2.3821)	0.3919 (1.3900)	1.1475 (8.2045)	0.8948 (0.7619)
WPLD	0.0486 (0.9968)	0.0293 (0.9791)	0.2476 (0.9717)	7.0524 (1.3770)	0.0028 (0.0011)	4.2835 (2.7236)	0.2677 (0.0675)

Table 7: The Y_1, Y_{1Pv}, Y_2, Y_{2Pv}, Y_3, Y_{3Pv}, MLEs, and SEs for daily UV-B radiation data

Name	Y_1 Y_{1Pv}	Y_2 Y_{2Pv}	Y_3 Y_{3Pv}	$\hat{\delta}$ $SE(\hat{\delta})$	$\hat{\lambda}$ $SE(\hat{\lambda})$	$\hat{\theta}$ $SE(\hat{\theta})$	$\hat{\beta}$ $SE(\hat{\beta})$
KMPCJD	0.1003 (0.9234)	0.0496 (0.8821)	0.4623 (0.7842)	0.0129 (0.0076)	2.3556 (0.2565)		
PCJD	0.1018 (0.9149)	0.0476 (0.8943)	0.4285 (0.8189)	2.2808 (0.273)	0.0182 (0.0115)		
KMRIWD	0.2611 (0.0335)	0.4720 (0.0463)	2.8563 (0.0328)	0.9621 (0.1149)	7.7587 (1.6682)		
KMBXD	0.1362 (0.6338)	0.0915 (0.6316)	0.7394 (0.5256)	3.4870 (0.9428)	0.1367 (0.0131)		

(Continued)

Table 7 (continued)

Name	Y_1 Y_{1Pv}	Y_2 Y_{2Pv}	Y_3 Y_{3Pv}	$\hat{\delta}$ $SE(\hat{\delta})$	$\hat{\lambda}$ $SE(\hat{\lambda})$	$\hat{\theta}$ $SE(\hat{\theta})$	$\hat{\beta}$ $SE(\hat{\beta})$
KMLoLD	0.1105 (0.8572)	0.0475 (0.8946)	0.5582 (0.687)	5.9548 (0.9214)	9.6602 (0.5053)		
KMGED	0.1647 (0.3901)	0.1690 (0.3378)	1.2587 (0.246)	13.9400 (4.9891)	0.3126 (0.0465)		
EGPLD	0.1301 (0.6899)	0.0782 (0.706)	0.6236 (0.6246)	2.4367 (0.0152)	0.0785 (0.0078)	0.0894 (0.0192)	1.8051 (0.4682)
WPLD	0.1234 (0.7506)	0.0620 (0.8053)	0.3716 (0.8755)	0.8678 (0.3518)	0.5099 (0.337)	0.0168 (0.0257)	1.6824 (1.3563)

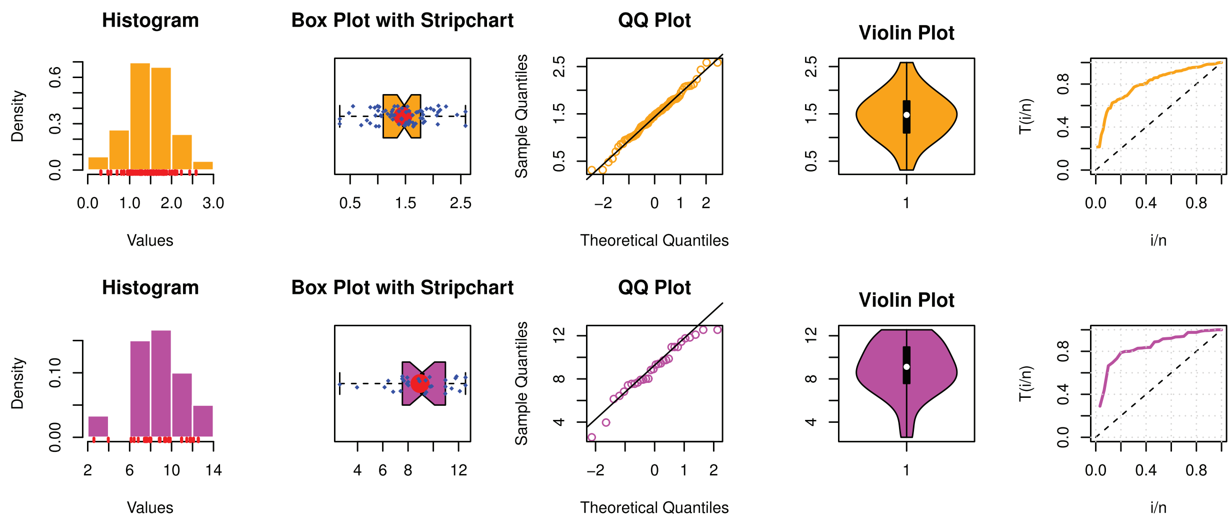

Figure 5: Some basic non-parametric plots for both engineering datasets

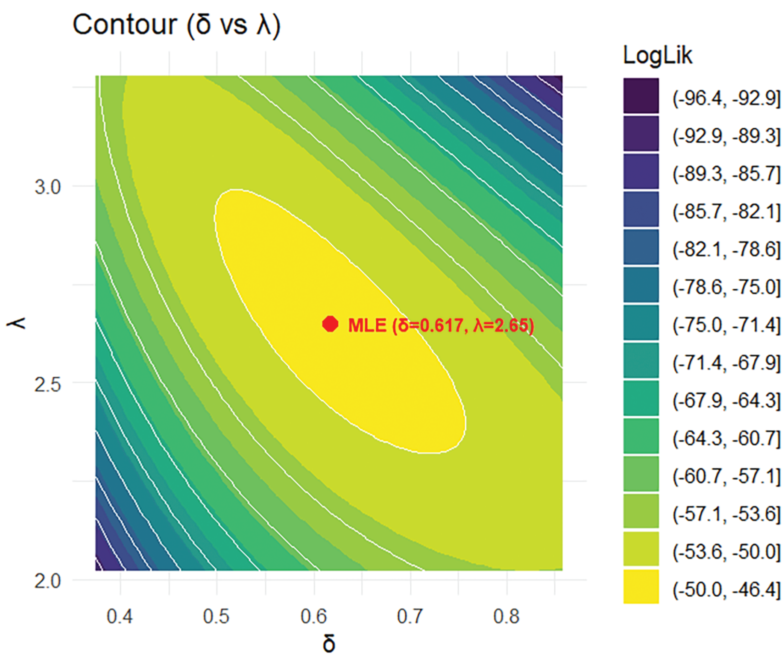

Figure 6: Countour plots of log-likelihood values with KMPCJD parameters for carbon fibers dataset

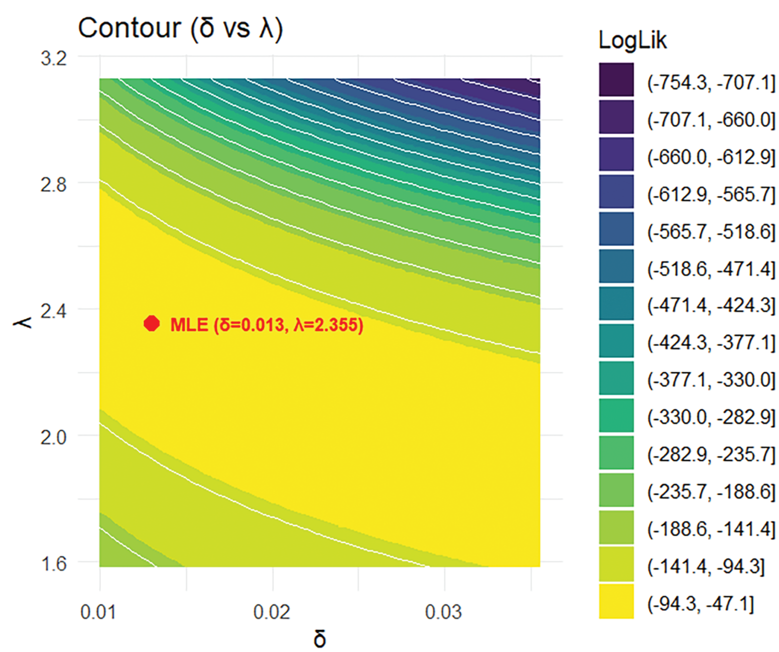

Figure 7: Countour plots of log-likelihood values with KMPCJD parameters for daily UV-B radiation dataset

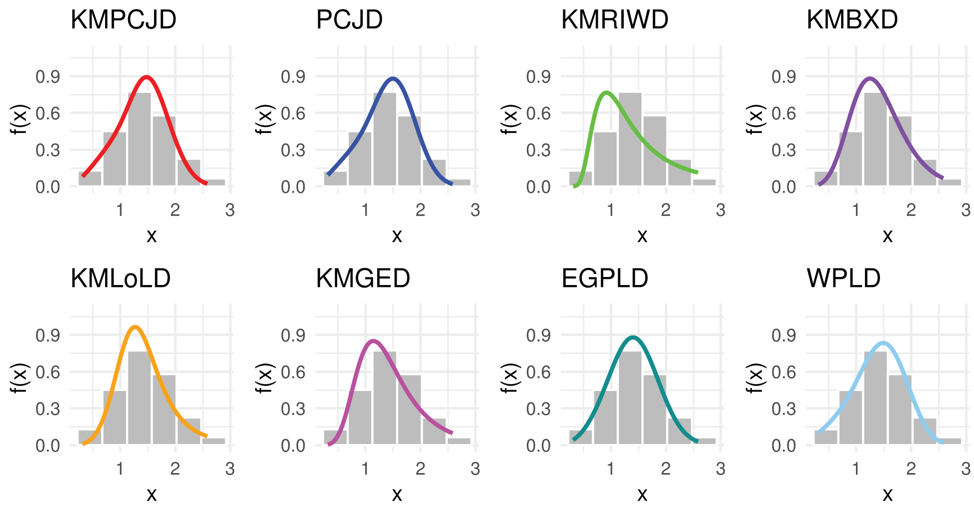

Figure 8: Estimated PDFs for the competing models for carbon fibers dataset

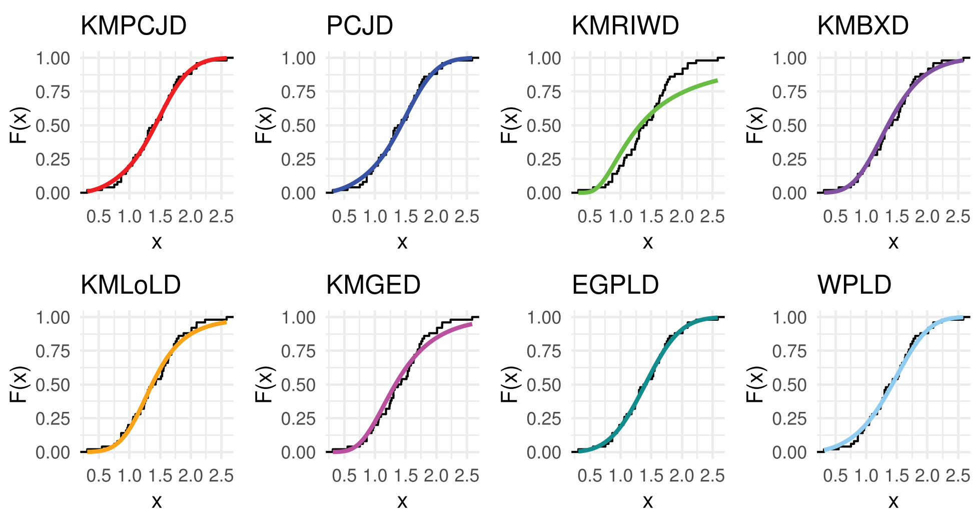

Figure 9: Estimated CDFs for the competing models for carbon fibers dataset

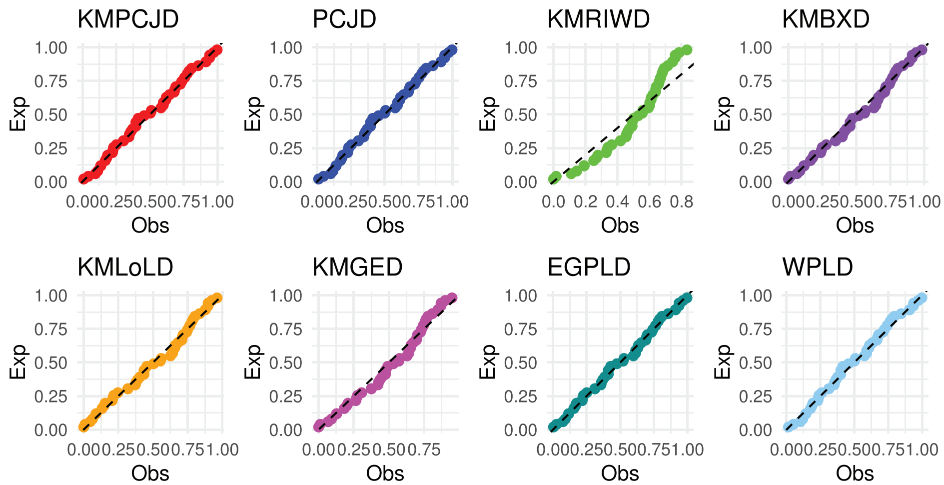

Figure 10: PP plots for the competing models for carbon fibers dataset

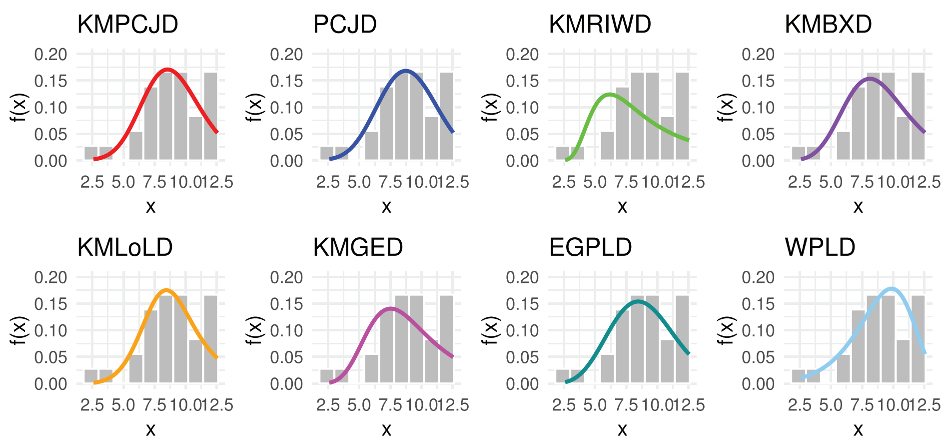

Figure 11: Estimated PDFs for the competing models for daily UV-B radiation dataset

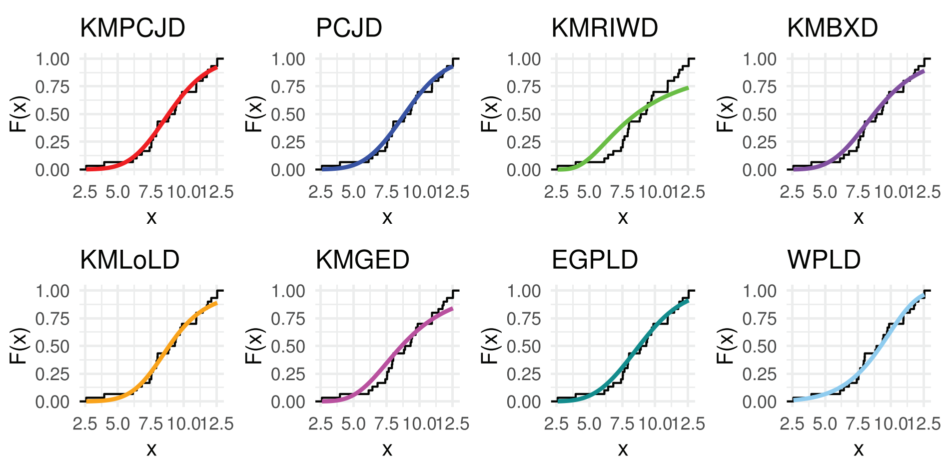

Figure 12: Estimated CDFs for the competing models for daily UV-B radiation dataset

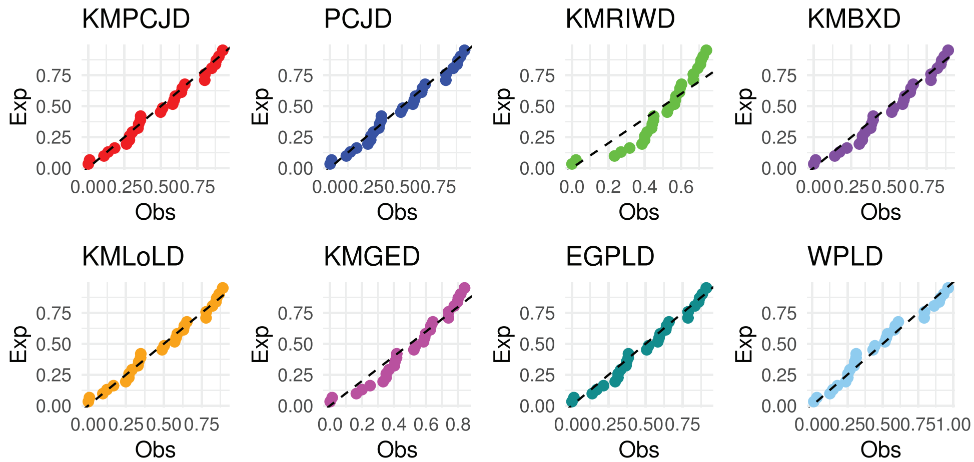

Figure 13: PP plots for the competing models for daily UV-B radiation dataset

7.2 Application to Disability in Saudi Arabia

In this subsection, we used five real data sets related to disability in KSA to show the importance and flexibility of the new suggested model according to Disability Statistics Publication 2023 in KSA [36].

The third dataset (Males)

This dataset presents the percentage distribution of severe disability types among males aged 18 years and above in Saudi Arabia. The reported percentages are:

Vision = 22.70, Hearing = 7.49, Mobility (Walking or Climbing Stairs) = 51.36, Mobility (Arm) = 3.86, Mobility (Hands and Fingers) = 0.60, Self-Care = 0.05, Communication = 1.22, Remembering = 2.87, Concentrating = 3.24, Remember and Concentrating Together = 5.49, Constant Anxiety = 0.79, Permanent Depression = 0.33.

The data show that the majority of severe disabilities among males are related to mobility (51.36%), followed by vision impairment (22.70%) and hearing disability (7.49%). Cognitive difficulties (remembering and concentrating) together account for more than 8% of cases, while mental health issues such as constant anxiety and permanent depression remain below 1.2%. This profile highlights the dominance of physical disabilities among males, particularly in mobility and vision.

The fourth dataset (Females)

This dataset presents the percentage distribution of severe disability types among females aged 18 years and above in Saudi Arabia. The reported percentages are:

Vision = 16.21, Hearing = 6.06, Mobility (Walking or Climbing Stairs) = 62.44, Mobility (Arm) = 3.82, Mobility (Hands and Fingers) = 0.50, Self-Care = 0.03, Communication = 1.11, Remembering = 2.87, Concentrating = 2.57, Remember and Concentrating Together = 3.70, Constant Anxiety = 0.46, Permanent Depression = 0.22.

The results indicate that mobility impairments are overwhelmingly dominant among females, representing 62.44% of all severe disability cases—more than ten percentage points higher than males. Vision and hearing disabilities are less prevalent compared to males, while cognitive impairments (remembering and concentrating) together contribute about 6.6%. These results emphasize the greater burden of mobility limitations among females, with comparatively lower rates of vision and hearing impairments.

The fifth dataset (Total Population)

This dataset represents the combined percentage distribution of severe disability types for the total population aged 18 years and above in Saudi Arabia. The reported percentages are:

Vision = 19.87, Hearing = 6.87, Mobility (Walking or Climbing Stairs) = 56.19, Mobility (Arm) = 3.84, Mobility (Hands and Fingers) = 0.55, Self-Care = 0.04, Communication = 1.17, Remembering = 2.87, Concentrating = 2.95, Remember and Concentrating Together = 4.71, Constant Anxiety = 0.64, Permanent Depression = 0.29.

At the population level, mobility-related disabilities are the most frequent (56.19%), followed by vision impairment (19.87%) and hearing impairment (6.87%). Cognitive disabilities (remembering, concentrating, or both) together represent over 7.5%, while psychological conditions (anxiety and depression) remain below 1%. This aggregate view provides essential evidence for national disability policy, infrastructure accessibility, and healthcare resource planning in Saudi Arabia

The MLEs and their SEs, as well as the Y_1, Y_{1Pv}, Y_2, Y_{2Pv}, Y_3, and Y_{3Pv} statistics are shown for the KMPCJD and the others in Tables 8–10, for the datasets. The histogram, violin plot, QQ plot, box plot with stripchart, and TTT plots, countour plots of log-likelihood values with KMPCJD parameters are shown in Figs. 14–17 for datasets. Figs. 18, 21 and 24 show the estimated PDFs, and Figs. 19, 22, and 25 show the estimated CDFs of the competing models for the datasets. Figs. 20, 23, and 26 also show the PP plots of the competing models.

Table 8: The Y_1, Y_{1Pv}, Y_2, Y_{2Pv}, Y_3, Y_{3Pv}, MLEs, and SEs for males data

Name	Y_1 Y_{1Pv}	Y_2 Y_{2Pv}	Y_3 Y_{3Pv}	$\hat{\delta}$ $SE(\hat{\delta})$	$\hat{\lambda}$ $SE(\hat{\lambda})$	$\hat{\theta}$ $SE(\hat{\theta})$	$\hat{\beta}$ $SE(\hat{\beta})$
KMPCJD	0.1233 (0.9826)	0.0287 (0.9842)	0.1925 (0.9928)	7.7756 (2.9077)	0.7041 (0.1453)		
PCJD	0.1358 (0.9585)	0.0352 (0.9625)	0.2281 (0.981)	0.6386 (0.1363)	8.5975 (2.8804)		
KMRIWD	0.1642 (0.8519)	0.0533 (0.8649)	0.3995 (0.8467)	0.2328 (0.0499)	0.3868 (0.1192)		
KMBXD	0.2190 (0.5416)	0.1035 (0.5755)	0.5334 (0.7095)	0.2289 (0.0621)	2.8612 (1.0498)		
KMUEHLD	0.1351 (0.9604)	0.0343 (0.9661)	0.2270 (0.9815)	2.2951 (1.1015)	0.6452 (0.1485)		
KMGED	0.1550 (0.8935)	0.0506 (0.8819)	0.3021 (0.9356)	0.5724 (0.1753)	6.0199 (3.1008)		

(Continued)

Table 8 (continued)

Name	Y_1 Y_{1Pv}	Y_2 Y_{2Pv}	Y_3 Y_{3Pv}	$\hat{\delta}$ $SE(\hat{\delta})$	$\hat{\lambda}$ $SE(\hat{\lambda})$	$\hat{\theta}$ $SE(\hat{\theta})$	$\hat{\beta}$ $SE(\hat{\beta})$
PXLD	0.1289 (0.9736)	0.0329 (0.9713)	0.2192 (0.9846)	6.0352 (2.3732)	0.6096 (0.1327)		
EGPLD	0.3132 (0.1521)	0.2414 (0.2004)	1.1685 (0.2789)	4.7474 (0.0025)	2.1853 (0.0025)	4.1443 (0.6193)	0.0624 (0.0181)
WPLD	0.1302 (0.971)	0.0362 (0.9583)	0.2493 (0.9708)	5.3526 (0.3489)	79.6059 (2.5125)	3.1837 (1.077)	0.1014 (0.0225)
PLD	0.1299 (0.9717)	0.0334 (0.9692)	0.2231 (0.9831)	0.6042 (0.134)	6.6148 (2.4449)		

Table 9: The Y_1, Y_{1Pv}, Y_2, Y_{2Pv}, Y_3, Y_{3Pv}, MLEs, and SEs for females data

Name	Y_1 Y_{1Pv}	Y_2 Y_{2Pv}	Y_3 Y_{3Pv}	$\hat{\delta}$ $SE(\hat{\delta})$	$\hat{\lambda}$ $SE(\hat{\lambda})$	$\hat{\theta}$ $SE(\hat{\theta})$	$\hat{\beta}$ $SE(\hat{\beta})$
KMPCJD	0.1536 (0.8995)	0.0397 (0.942)	0.2538 (0.9683)	7.2924 (2.5953)	0.6465 (0.1319)		
PCJD	0.1642 (0.8518)	0.0454 (0.9122)	0.2910 (0.944)	0.5843 (0.1235)	8.1179 (2.61)		
KMRIWD	0.1802 (0.7688)	0.0644 (0.796)	0.4321 (0.8134)	0.2213 (0.0477)	0.3845 (0.1193)		
KMBXD	0.2542 (0.3584)	0.1431 (0.416)	0.7351 (0.5271)	0.2014 (0.0539)	2.3604 (0.9042)		
KMUEHLD	0.1710 (0.8183)	0.0500 (0.8854)	0.3232 (0.9184)	2.0246 (0.9271)	0.5828 (0.134)		
KMGED	0.2014 (0.6447)	0.0728 (0.7438)	0.4226 (0.8233)	0.5064 (0.1522)	5.3675 (2.8687)		
PXLD	0.1575 (0.8829)	0.0415 (0.9328)	0.2709 (0.9579)	5.7187 (2.1715)	0.5602 (0.12)		
EGPLD	0.3146 (0.1489)	0.2526 (0.1854)	1.2391 (0.2525)	4.4520 (0.0033)	1.2972 (0.0033)	3.4997 (0.0068)	0.0569 (0.0165)
WPLD	0.1792 (0.7743)	0.0609 (0.8181)	0.3565 (0.8886)	4.9215 (0.0026)	24.0088 (0.1587)	3.1343 (1.0325)	0.1013 (0.022)
PLD	0.1585 (0.8783)	0.0421 (0.9297)	0.2758 (0.9547)	0.5545 (0.1211)	6.2821 (2.2392)		

Table 10: The Y_1, Y_{1Pv}, Y_2, Y_{2Pv}, Y_3, Y_{3Pv}, MLEs, and SEs for total data

Name	Y_1 Y_{1Pv}	Y_2 Y_{2Pv}	Y_3 Y_{3Pv}	$\hat{\delta}$ $SE(\hat{\delta})$	$\hat{\lambda}$ $SE(\hat{\lambda})$	$\hat{\theta}$ $SE(\hat{\theta})$	$\hat{\beta}$ $SE(\hat{\beta})$
KMPCJD	0.1332 (0.9647)	0.0338 (0.9676)	0.2183 (0.9849)	7.5615 (2.7659)	0.6801 (0.1396)		
PCJD	0.1449 (0.9319)	0.0400 (0.9405)	0.2548 (0.9677)	0.6159 (0.1308)	8.3839 (2.7575)		
KMRIWD	0.1775 (0.7837)	0.0583 (0.8341)	0.4147 (0.8313)	0.2283 (0.049)	0.3858 (0.1192)		
KMBXD	0.2356 (0.4501)	0.1203 (0.5002)	0.6190 (0.6266)	0.2169 (0.0585)	2.6343 (0.9831)		
KMUEHLD	0.1475 (0.9228)	0.0410 (0.9356)	0.2650 (0.9617)	2.1793 (1.0248)	0.6193 (0.1423)		
KMGED	0.1703 (0.8219)	0.0599 (0.8239)	0.3501 (0.8946)	0.5448 (0.1656)	5.7507 (3.0059)		
PXLD	0.1369 (0.9558)	0.0370 (0.9545)	0.2412 (0.9749)	5.8940 (2.2818)	0.5889 (0.1272)		
EGPLD	0.2918 (0.2122)	0.2070 (0.256)	1.0430 (0.3339)	4.6340 (0.003)	1.8556 (0.003)	4.5000 (0.0066)	0.0572 (0.0166)
WPLD	0.1348 (0.961)	0.0369 (0.9551)	0.2493 (0.9708)	4.6956 (0.0029)	2.9993 (0.002)	5.4977 (2.1357)	0.1293 (0.0278)
PLD	0.1380 (0.9529)	0.0376 (0.9517)	0.2456 (0.9727)	0.5833 (0.1284)	6.4659 (2.3513)		

Based on the results in Tables 8–10, it is clear that the KMPCJD exhibits the best modelling ability among the models investigated. This is demonstrated by the lowest Y_1, Y_2, and Y_3 values and the largest Y_{1Pv}, Y_{2Pv}, and Y_{3Pv}. Figs. 18–26 show how well our distribution was fitted by the real data.

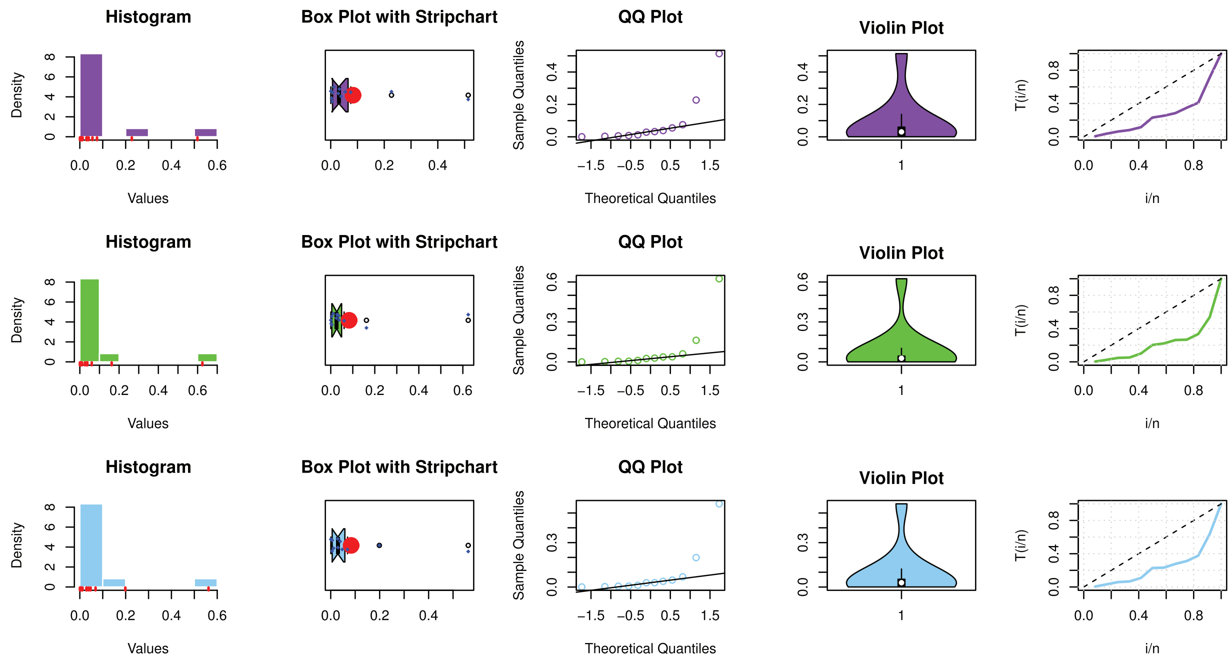

Figure 14: Some basic non-parametric plots for Disability datasets

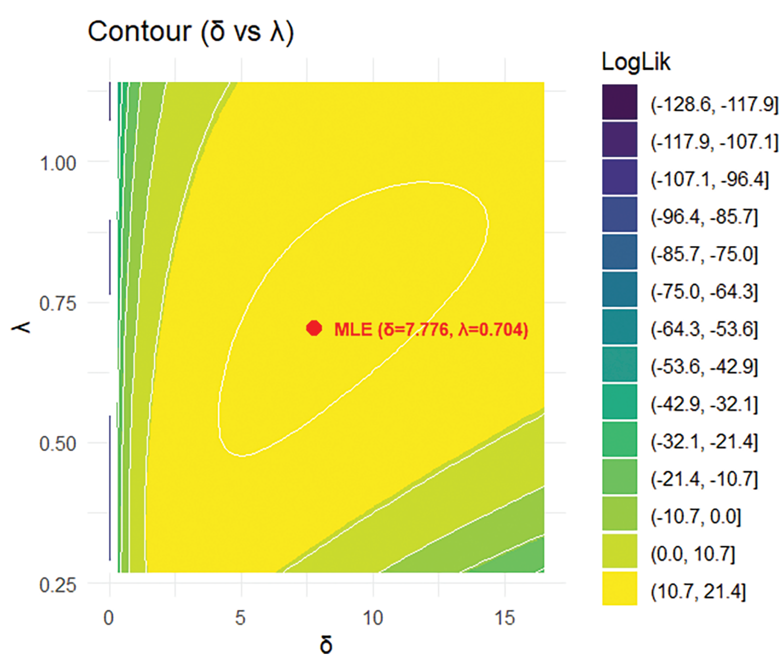

Figure 15: Countour plots of log-likelihood values with KMPCJD parameters for males dataset

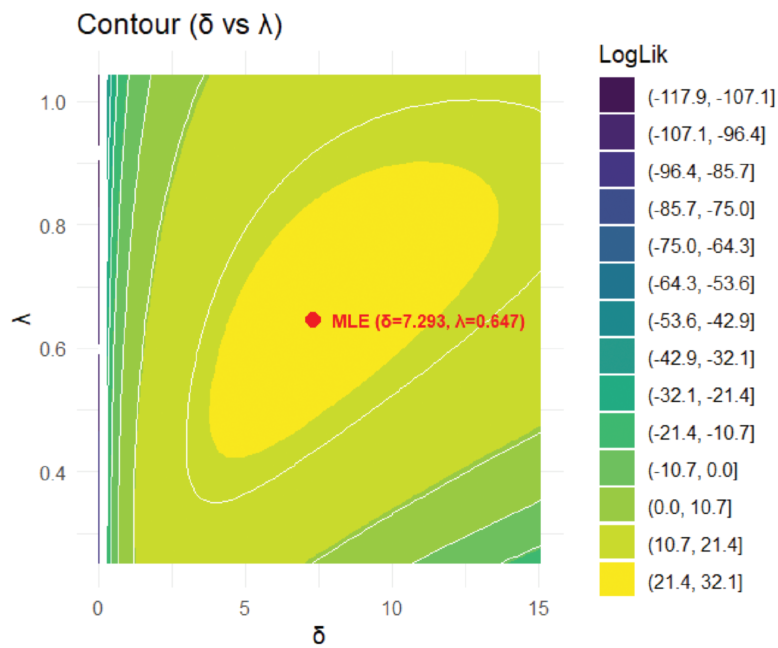

Figure 16: Countour plots of log-likelihood values with KMPCJD parameters for females dataset

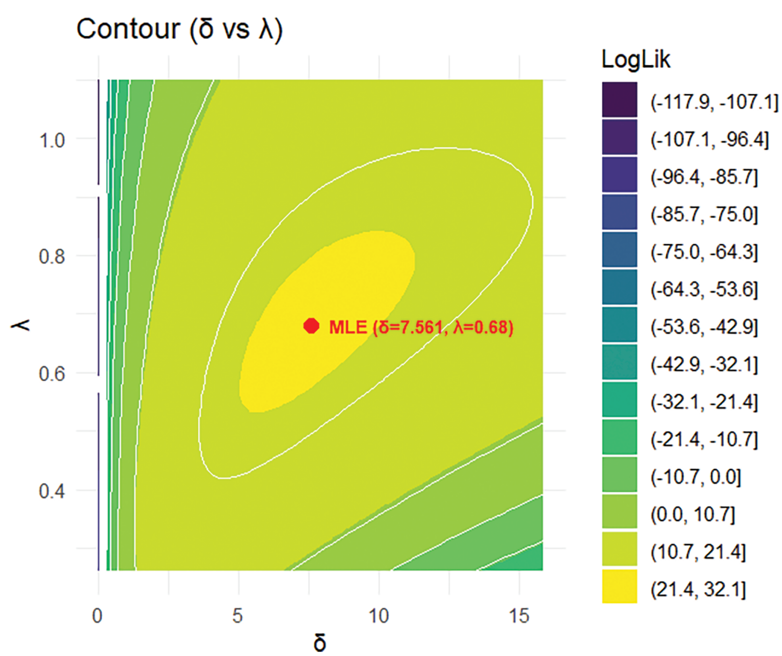

Figure 17: Countour plots of log-likelihood values with KMPCJD parameters for total dataset

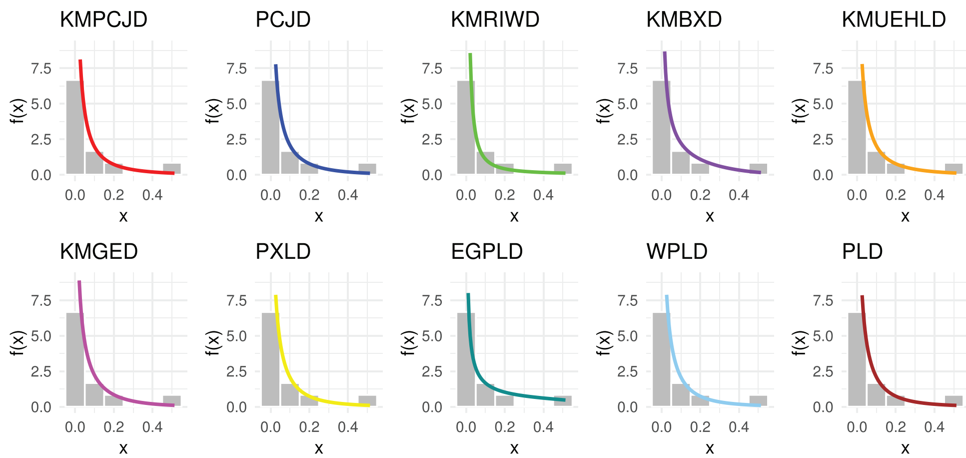

Figure 18: Estimated PDFs for the competing models for males dataset

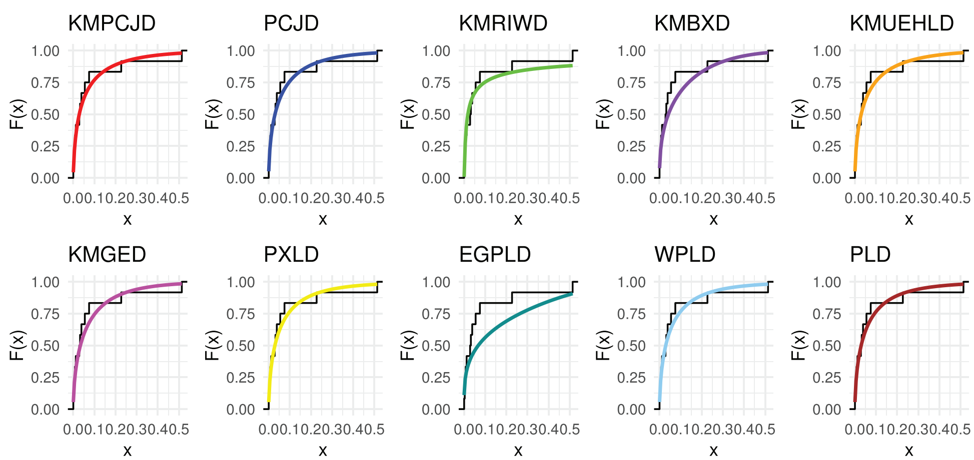

Figure 19: Estimated CDFs for the competing models for males dataset

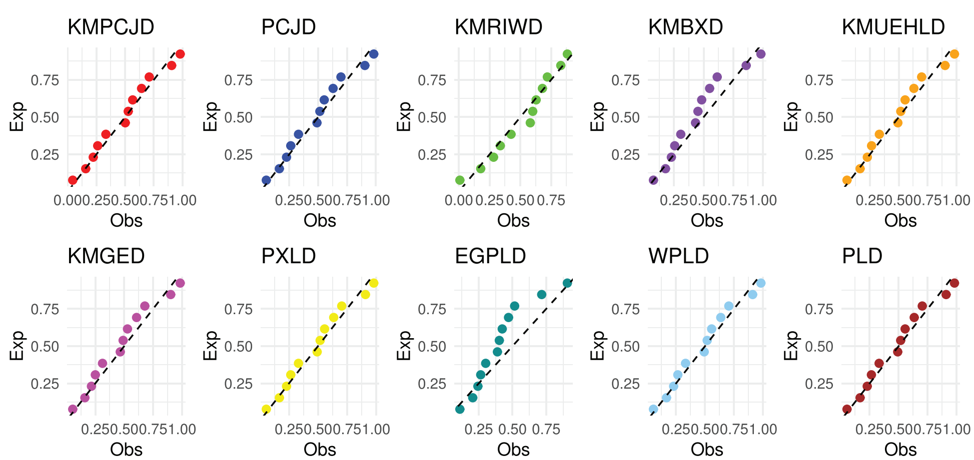

Figure 20: PP plots for the competing models for males dataset

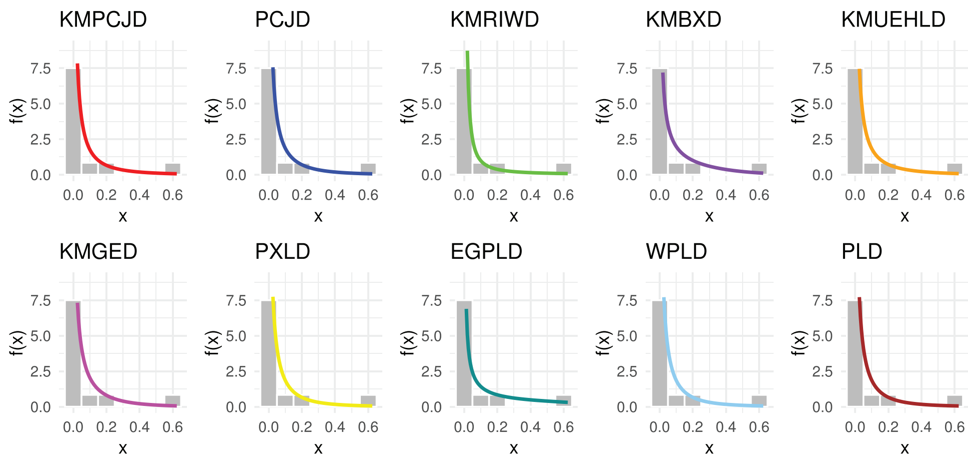

Figure 21: Estimated PDFs for the competing models for females dataset

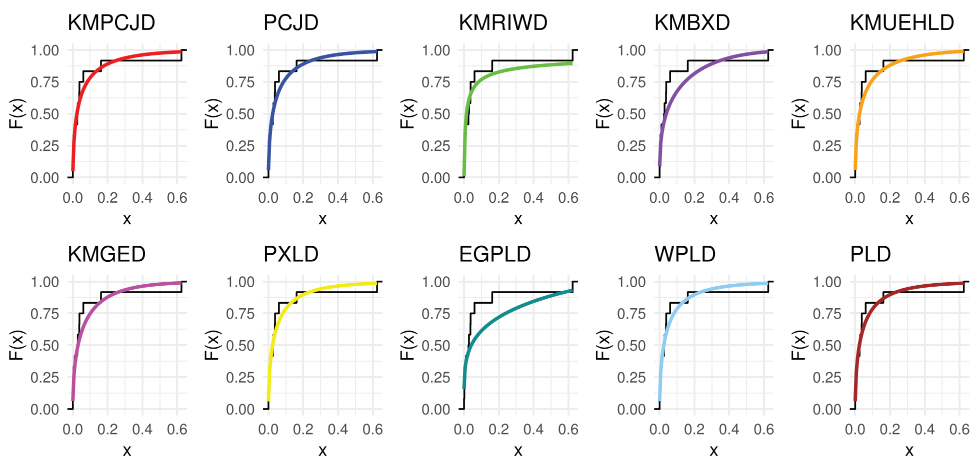

Figure 22: Estimated CDFs for the competing models for females dataset

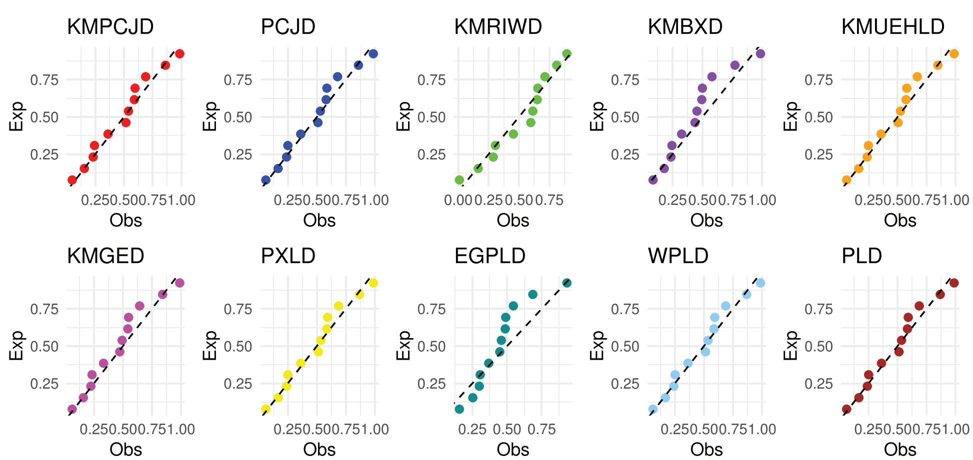

Figure 23: PP plots for the competing models for females dataset

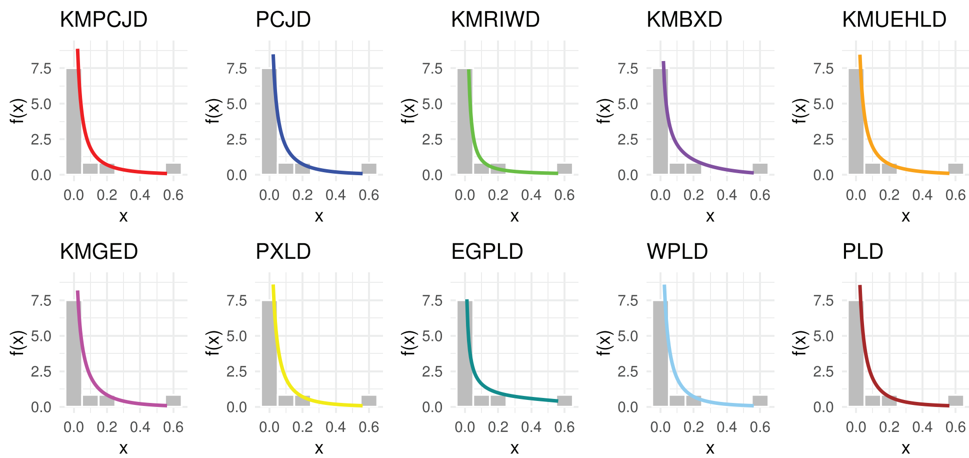

Figure 24: Estimated PDFs for the competing models for total dataset

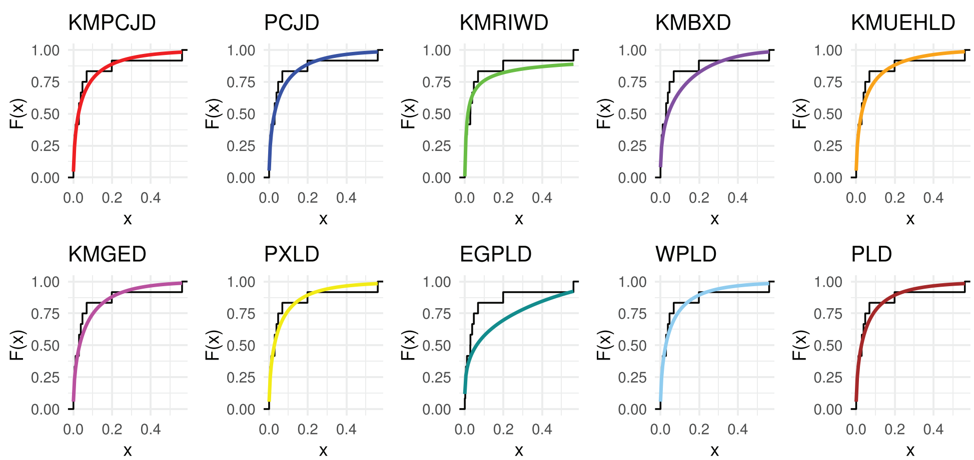

Figure 25: Estimated CDFs for the competing models for total dataset

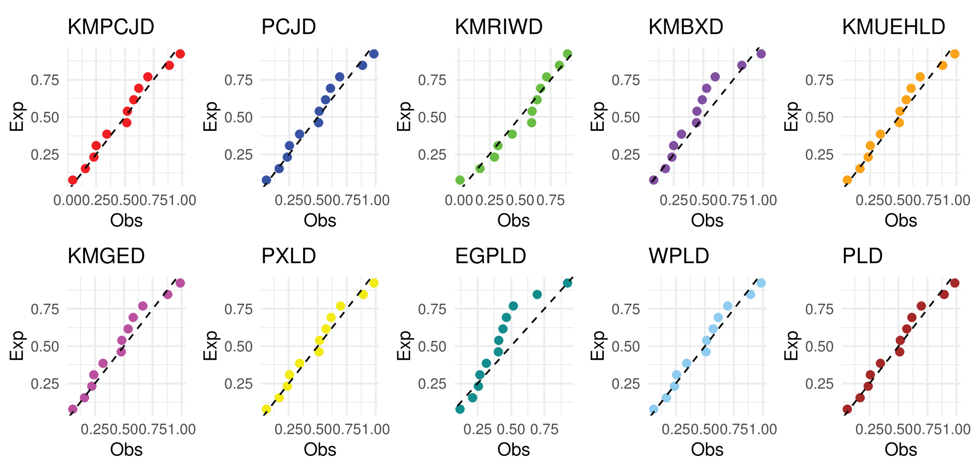

Figure 26: PP plots for the competing models for total dataset

8 Concluding Remarks

This article introduces the Kavya-Manoharan power Chris-Jerry distribution (KMPCJD), a modified version of the power Chris-Jerry distribution (PCJD) that use the Kavya-Manoharan approach to address these challenges. The probability density curves of KMPCJD indicate its practical utility in the analysis of engineering and disability data in Saudi Arabia. Researchers possess considerable versatility in formulating statistical models for the study of disability issues, as the hazard rate function (HRF) for KMPCJD may display J-shaped, increasing, and decreasing trends. Furthermore, other notable characteristics of the KMPCJD are computed, which include moments, reliability metrics, moment generating function, and order statistics. Using data on engineering and disability challenges, we estimate the parameters of KMPCJD and employ traditional and Bayesian methodologies to evaluate their reliability and HRF under hybrid-censored frameworks. Asymptotic confidence intervals are computed. The proposed distribution was evaluated using five datasets related to engineering and disability concerns in Saudi Arabia. The proposed distribution was evaluated using three datasets related to engineering and disability concerns in Saudi Arabia. The KMPCJD exhibited superior goodness of fit compared to several models, including the Kavya Manoharan Rayleigh inverted Weibull distribution, Kavya Manoharan Burr X distribution, exponentiated generalized power Lindley distribution, Weibull power Lindley distribution, power Lindley distribution, Kavya Manoharan generalized exponential distribution, power XLindley distribution, Kavya Manoharan unit exponentiated half logistic distribution, and PCJD. The KMPCJD is recommended for data modeling in fields such as engineering and disability challenges due to its excellent fit capabilities. The limitation of this study lies in that we study only the univariate case of KMPCJD. This reason opens the doors for researchers to study the extension of KMPCJD to regression models or multivariate settings in their future work.

Acknowledgement: The authors extend their appreciation to the King Salman Center for Disability Research for funding this work through Research Group No. KSRG-2024-159.

Funding Statement: The authors extend their appreciation to the King Salman Center for Disability Research for funding this work through Research Group No. KSRG-2024-159.

Author Contributions: Conceptualization, Abdullah Ali H. Ahmadini and Mohammed Elgarhy; methodology, Abdullah Ali H. Ahmadini and Mohammed Elgarhy; software, Ahmed R. El-Saeed; validation, Mohammed Elgarhy, Abdullah Ali H. Ahmadini and Ahmed R. El-Saeed; formal analysis, Ehab M. Almetwally; investigation, Abdullah Ali H. Ahmadini; resources, Mohammed Elgarhy; data curation, Ahmed R. El-Saeed; writing—original draft preparation, Abdullah Ali H. Ahmadini, Ahmed R. El-Saeed, Ehab M. Almetwally and Mohammed Elgarhy; writing—review and editing, Abdullah Ali H. Ahmadini, Ahmed R. El-Saeed, Ehab M. Almetwally and Mohammed Elgarhy; visualization, Abdullah Ali H. Ahmadini; supervision, Mohammed Elgarhy; project administration, Mohammed Elgarhy; funding acquisition, Ahmed R. El-Saeed. All authors reviewed the results and approved the final version of the manuscript.

Availability of Data and Materials: Data available on request from the authors.

Ethics Approval: Not applicable.

Conflicts of Interest: The authors declare no conflicts of interest to report regarding the present study.

References

1. Onyekwere CK, Obulezi OJ. Chris-Jerry distribution and its applications. Asian J Probab Stat. 2022;20:16–30. doi:10.9734/ajpas/2022/v20i130480.
2. Obulezi OJ, Anabike IC, Okoye GC, Igbokwe CP, Etaga HO, Onyekwere CK. The Kumaraswamy Chris-Jerry distribution and its applications. J Xidian Univ. 2023;17(6):575–91. doi:10.37896/jxu17.6/061.
3. Innocent CF, Frederick OA, Udofia EM, Obulezi OJ, Igbokwe CP. Estimation of the parameters of the power size biased Chris-Jerry distribution. Int J Innov Sci Res Technol. 2023;8(5):423–36.
4. Obulezi OJ, Anabike IC, Oyo OG, Igbokwe CP. Marshall-Olkin Chris-Jerry distribution and its applications. Int J Innov Sci Res Technol. 2023;8(5):522–33.
5. Ezeilo CI, Sidney OI, Umeh EU, Onyekwere CK. On power Chris-Jerry distribution: properties and parameter estimation methods. Asian J Probab Stat. 2023;25(3):29–44. doi:10.9734/ajpas/2023/v25i3562.
6. Oramulu DO, Igbokwe CP, Anabike IC, Etaga HO, Obulezi OJ. Simulation study of the Bayesian and non-Bayesian estimation of a new lifetime distribution parameters with increasing hazard rate. Asian Res J Math. 2023;19(9):183–211. doi:10.9734/arjom/2023/v19i9711.
7. Chinedu EQ, Chukwudum QC, Alsadat N, Obulezi OJ, Almetwally EM, Tolba AH. New lifetime distribution with applications to single acceptance sampling plan and scenarios of increasing hazard rates. Symmetry. 2023;15(10):1881. doi:10.3390/sym15101881.
8. Kavya P, Manoharan M. Some parsimonious models for lifetimes and applications. J Stat Comput Simul. 2021;91(18):3693–708. doi:10.1080/00949655.2021.1946064.
9. Kavya P, Manoharan M. A new lifetime model for non-monotone failure rate data. J Indian Soc Probab Stat. 2023;24(2):211–41. doi:10.1007/s41096-023-00152-x.
10. Al-Nefaie AH. Applications to bio-medical data and statistical inference for a Kavya-Manoharan log-logistic model. J Radiat Res Appl Sci. 2023;16(1):100523. doi:10.1016/j.jrras.2023.100523.
11. Alrashidi A. Arctan Kavya-Manoharan-G class of distributions with modelling in different fields. Adv Appl Stat. 2024;91(4):393–420. doi:10.17654/0972361724021.
12. Shafiq A, Sindhu TN, Riaz MB, Hassan MK, Abushal TA. A statistical framework for a new Kavya-Manoharan Bilal distribution using ranked set sampling and simple random sampling. Heliyon. 2024;10(9):e30762. doi:10.1016/j.heliyon.2024.e30762.
13. Mahran H, Mansour MM, Abd Elrazik EM, Afify AZ. A new one-parameter flexible family with variable failure rate shapes: properties, inference, and real-life applications. AIMS Math. 2024;9(5):11910–40. doi:10.3934/math.2024582.
14. Haj Ahmad H, Almetwally EM, Rabaiah A, Ramadan DA. Statistical analysis of alpha power inverse Weibull distribution under hybrid censored scheme with applications to ball bearings technology and biomedical data. Symmetry. 2023;15(1):161. doi:10.3390/sym15010161.
15. Elsherpieny EA, Abdel-Hakim A. Statistical analysis of alpha-power exponential distribution using unified hybrid censored data and its applications. Comput J Math Stat Sci. 2025;4(1):283–315. doi:10.21608/cjmss.2025.346134.1094.
16. Abdelwahab MM, Ghorbal AB, Hassan AS, Elgarhy M, Almetwally EM, Hashem AF. Classical and Bayesian inference for the Kavya-Manoharan generalized exponential distribution under generalized progressively hybrid censored data. Symmetry. 2023;15(6):1193. doi:10.3390/sym15061193.
17. Hassan AS, Hagag AE, Metwally N, Sery OH. Statistical analysis of inverse Weibull based on step-stress partially accelerated life tests with unified hybrid censoring data. Comput J Math Stat Sci. 2025;4(1):162–85. doi:10.21608/cjmss.2024.319502.1072.
18. Helmy BA, Hassan AS, El-Kholy AK. Analysis of uncertainty measure using unified hybrid censored data with applications. J Taibah Univ Sci. 2021;15(1):1130–43. doi:10.1080/16583655.2021.2022901.

19. Ramses El-Saeed A, Abdellatif AD. Point and interval estimation of reliability and entropy for generalized exponential distribution under generalized type-II hybrid censoring scheme. Comput J Math Stat Sci. 2025;4(1):96–138. doi:10.21608/cjmss.2024.327558.1078.
20. Husain QN, Qaddoori AS, Noori NA, Abdullah KN, Suleiman AA, Balogun OS. New expansion of Chen distribution according to the nitrosophic logic using the Gompertz family. Innov Stat Probab. 2025;1(1):60–75. doi:10.64389/isp.2025.01105.
21. Saboor A, Jamal F, Shafq S, Mumtaz R. On the versatility of the unit logistic exponential distribution: capturing bathtub, upside-down bathtub, and monotonic hazard rates. Innov Stat Probab. 2025;1(1):28–46. doi:10.64389/isp.2025.01102.
22. Hassan A, Khalil A, Nagy H. Versatile extension of the unit Gompertz: efficient estimation and application. Gazi Univ J Sci. 2025;38(3):1540–64. doi:10.35378/gujs.1541941.
23. Greene WH. Econometric analysis. 4th ed. New York, NY, USA: Prentice-Hall; 2000.
24. Cheng RCH, Amin NAK. Estimating parameters in continuous univariate distributions with a shifted origin. J R Stat Soc B. 1983;45(3):394–403. doi:10.1111/j.2517-6161.1983.tb01268.x.
25. Gemeay AM, Moakofi T, Balogun OS, Ozkan E, Hossain MM. Analyzing real data by a new heavy-tailed statistical model. Mod J Stat. 2025;1(1):1–24. doi:10.64389/mjs.2025.01108.
26. Dey S, Singh S, Tripathi YM, Asgharzadeh A. Estimation and prediction for a progressively censored generalized inverted exponential distribution. Stat Methodol. 2016;32(4):185–202. doi:10.1016/j.stamet.2016.05.007.
27. Henningsen A, Toomet O. maxLik: a package for maximum likelihood estimation in R. Comput Stat. 2011;26(3):443–58. doi:10.1007/s00180-010-0217-1.
28. Plummer M, Best N, Cowles K, Vines K. Package ‘coda’ [Internet]. [cited 2025 Jan 25]. Available from: http://cran.r-project.org/web/packages/coda/coda.pdf.
29. Elgarhy M, Kayid M, Johannssen A, Elsehetry M. Survival analysis based on an enhanced Rayleigh-inverted Weibull model. Heliyon. 2024;10(16):e35851. doi:10.1016/j.heliyon.2024.e35851.
30. Hassan OHM, Elbatal I, Al-Nefaie AH, Elgarhy M. On the Kavya-Manoharan-Burr X model: estimations under ranked set sampling and applications. J Risk Financ Manag. 2022;16(1):19. doi:10.3390/jrfm16010019.
31. MirMostafaee SMTK, Alizadeh M, Altun E, Nadarajah S. The exponentiated generalized power Lindley distribution: properties and applications. Appl Math J Chin Univ. 2019;34:127–48. doi:10.1007/s11766-019-3515-6.
32. Bourguignon M, Silva RB, Cordeiro GM. The Weibull-G family of probability distributions. J Data Sci. 2014;12(1):53–68.
33. Ghitany ME, Al-Mutairi DK, Balakrishnan N, Al-Enezi LJ. Power Lindley distribution and associated inference. Comput Stat Data Anal. 2013;64(9):20–33. doi:10.1016/j.csda.2013.02.026.
34. Alotaibi N, Al-Moisheer AS, Hassan AS, Elbatal I, Alyami SA, Almetwally EM. Epidemiological modeling of COVID-19 data with advanced statistical inference based on type-II progressive censoring. Heliyon. 2024;10(18):e36774. doi:10.1016/j.heliyon.2024.e36774.
35. Raqab MZ, Madi MT, Kundu D. Estimation of $P(Y<X)$ for the three-parameter generalized exponential distribution. Commun Stat Theory Methods. 2008;37(18):2854–64. doi:10.1080/03610920802162664.
36. General Authority for Statistics. Disability statistics. Saudi Arabia: General Authority for Statistics; 2025 [Internet]. [cited 2025 Mar 10]. Available from: https://www.stats.gov.sa/statistics-tabs/-/categories/123728?tab=436312&category=123728.